Mesoscale cortex-wide neural dynamics predict goal-directed, but not random actions in mice several seconds prior to movement

*Mitelut C.[1,2,3,5], Zhang Y[4], Sekino Y[1,2], Boyd J[1,2], Bolanos F[1,2], Swindale N.V.[3], Silasi G[6], +Saxena S[4], *+Murphy T.H.[1,2]

1 - Department of Psychiatry, Kinsmen Laboratory of Neurological Research, Univ of British Columbia
2 - Djavad Mowafaghian Centre for Brain Health, University of British Columbia
3 - Department of Ophthalmology and Visual Sciences, University of British Columbia
4 - Department of Engineering, University of Florida
5 - Biozentrum, Centre for Molecular Life Sciences, University of Basel
6 - Department of Cellular and Molecular Medicine, University of Ottawa

+ Equal contribution senior author
* Correspondence to: C Mitelut, T Murphy
Address: South Lab, 2550 Willow Street, Vancouver, BC, Canada V5Z 3N9
E-mail: cat@alumni.ubc.ca; thmurphy@mail.ubc.ca

Keywords: behavior prediction, behavior forecasting, voluntary behavior, self-initiated behavior, volition neuroscience, free will

Abbreviated title: Predicting mouse self-initiated behavior from neural activity

Number of pages: 83
Number of main figures: 8
Number of words: 11737
- **Abstract:** 254

Conflict of Interest: None
Acknowledgements: This work was supported by: Canadian Institutes of Health Research (CIHR) Operating Grant MOP-15360 and National Science and Engineering Research Council of Canada 178702; Canadian Institutes of Health Research (CIHR) Operating Grant MOP-12675 and Foundation Grant FDN-143209 to T.H.M. We thank Pumin Wang, Cindy Jiang for surgical assistance; Jeff LeDue for technical assistance. We also thank Kenny Kay, Xuexin Wei and Allen Chan for comments on the initial manuscript.

ABSTRACT

Volition - the sense of control or agency over one's voluntary actions - is widely recognized as the basis of both human subjective experience and natural behavior in non-human animals. Several human studies have found peaks in neural activity preceding voluntary actions, e.g. the readiness potential (RP), and some have shown upcoming actions could be decoded even before awareness. Others propose that random processes underlie and explain pre-movement neural activity. Here we seek to address these issues by evaluating whether pre-movement neural activity in mice contains structure beyond that present in random neural activity. Implementing a self-initiated water-rewarded lever pull paradigm in mice while recording widefield [Ca++] neural activity we find that cortical activity changes in variance seconds prior to movement and that upcoming lever pulls could be predicted between 3 to 5 seconds (or more in some cases) prior to movement. We found inhibition of motor cortex starting at approximately -5sec prior to lever pulls and activation of motor cortex starting at approximately 2sec prior to a random unrewarded left limb movement. We show that mice, like humans, are biased towards commencing self-initiated actions during specific phases of neural activity but that the pre-movement neural code changes over time in some mice and is widely distributed as behavior prediction improved when using all vs single cortical areas. These findings support the presence of structured multi-second neural dynamics preceding self-initiated action beyond that expected from random processes. Our results also suggest that neural mechanisms underlying self-initiated action could be preserved between mice and humans.

INTRODUCTION

Over the past several decades studies of volitional, i.e. free and voluntary, action in humans using self-initiated (i.e. uncued) behaviors such as flexing a finger or pressing a button have shown that prior to movement there is a gradual increase in scalp electroencephalography (EEG) signal over pre- and supplementary-motor-area (pre-SMA and SMA, respectively; Ball et al., 1999; Cunnington et al 2002). This increase in activity is known as the "readiness potential" (RP; Kornhuber & Deecke, 1964, 1965; Deecke, Grözinger, & Kornhuber, 1976; Deecke & Kornhuber, 1978; Libet 1983; Shibasaki and Hallett 2006) and has received increasing attention with some interpretations that it is evidence that voluntary decisions might be made prior to awareness with several studies replicating and extending the original work (Haggard & Eimer, 1999; Schlegel et al., 2013; Sirigu et al., 2004; Alexander et al. 2016). Additionally, single neuron physiology studies have also shown a significant increase (or decrease) in the firing rate of single neurons in SMA and pre-SMA (as well as anterior cingulate cortex; ACC) prior to movement (Fried et al 2011). In parallel, human functional magnetic resonance imaging (fMRI) studies have shown that upcoming behaviors could be decoded up to several seconds prior to movement (Soon et al 2008; 2013; Bode et al 2011; Colas and Hsieh 2014). The role of pre-movement neural activity in voluntary behavior is the subject of active debates on human decision making including free will (Jahanshahi and Hallett, 2003; Lang, 2003; Shibasaki and Hallett, 2006; Haggard, 2008; Klemm, 2010; Custers and Aarts, 2010; Schurger 2012; Deecke 2012; Guggisberg and Mottaz, 2013; Bode et al., 2014; Maoz et al 2015; Lavazza 2016; Schurger et al 2016). These debates on the neural genesis of voluntary action are further complicated as other studies have shown volitional actions are more likely to occur during certain phases of breathing (e.g. exhalation; Park et al 2020), or phases in cumulative neural activity (ie. the crest in slow cortical potential - SCP; Schmidt et al 2016) which have no immediately obvious connections to volitional intent, awareness, neural noise, or external stimuli or cues.

Although some have called for better-designed self-initiated behavior studies (e.g. Mudrik et al 2020), it remains challenging to implement them in humans especially in cue-free paradigms. First, neuroanatomically precise high-temporal and spatial precision recordings from many cortical areas are rare in humans (though some limited studies exist, e.g. Fried et al 2011). Second, obtaining statistically sufficient numbers of trials (i.e. tracking behaviors for days or weeks; see Bode et al 2014 for a discussion) of higher-value salient actions (e.g. important decisions that are made naturally outside of laboratory environments) is not yet possible in humans. Additionally, human laboratory protocols for volitional studies (e.g., the subject being told to act freely in a study) may result in instructed - rather than free behavior - and there are concerns about whether human subjects can act randomly (Lages et al 2013) or otherwise carry out balanced behaviors (e.g. randomly pressing left vs. right button) in voluntary behavior paradigms (Bode et al 2014). An alternative approach to studying self-initiated action is to characterize the neural correlates of voluntary action and removing the requirement for reporting intent or awareness altogether (similar to some human studies, e.g. Soon et al 2008, 2011; Bode et al 2011). This avoids some of the challenges of human paradigms and makes it possible to implement non-human animal models where more ethologically valuable actions could be available (i.e. food or water seeking behaviors) and higher resolution intracranial neural recordings can be made during hundreds or thousands of trials. There is evidence to support this direction as several non-human studies have identified structure - or increases - in pre-movement neural activity in non-human primates (Romo and Schultz 1986; 1990; Coe et al., 2002; Lee and Assad 2003; Maimon and Assad 2006; Ding and Hikosaka, 2006), rodents (Hyland 1998; Isomura et al 2013; Murakami et al 2014), crayfish (Kagaya and Takahata, 2010), zebrafish (Lin et al 2020). However, none of these studies were designed to - nor report - the neural structure of either voluntary or self-initiated actions and they do not evaluate the predictive relationship between pre-movement cortical neural activity and self-initiated behaviors.

Here we report results obtained from a self-initiated behavior paradigm targeting the decoding of future body movement and rewarded actions from neural activity in mice. Using a self-initiated task and widefield [Ca++] cortical imaging (Silasi et al 2016; Vanni and Murphy 2014) we tracked both water rewarded lever pull behavior of water deprived mice as well as spontaneous body movements. We gathered hundreds to thousands of self-initiated actions over months of recordings and collected neural activity from several cortical areas. We find that both self-initiated water rewarded lever pulls and spontaneous body movements could be decoded above chance a few to several seconds prior to movement initiation from neural activity. We show the self-initiated movement neural code is distributed across multiple cortical areas and additionally replicate and extend several findings from human studies. Our study is in line with accounts of pre-movement neural activity having temporal and spatial structure beyond that present in random neural dynamics and supports a causal role between pre-movement neural activity and action that is on the scale of several seconds prior to action.

RESULTS

Fig 1: Tracking and decoding self-initiated behaviors from widefield neural activity in mice

Figure 1 here

Several studies of voluntary actions, such as finger or wrist movements, in humans have identified an increase in scalp EEG signal over SMA and pre-SMA - known as the RP - occurring 0.5sec to 1.5sec prior to movement and in some cases awareness of movement (Fig 1a, b; Kornhubber and Deecke 1964, 1965; Libet et al 1983; Ball et al., 1999; Cunnington et al 2002).

Self-initiated movements in mice are preceded by stereotyped neural activity changes several seconds prior to movement. We developed an analogous self-initiated behavior paradigm in six mice (M1-M6) to characterize pre-movement neural activity while recording widefield [Ca++] activity from cortex (Figure 1c, d, Figure 1 - figure supplement 1, 2; see also Methods). Mice were headfixed and trained to perform a self-initiated lever-pull to receive a water reward without sensory cues or stimuli. Four of six mice learned the lever lockout period of 3 sec (Figure 1 - figure supplement 2 shows peaks at 3-sec in the inter-lever-pull intervals in mice M3-M6) and four of six mice learned to pull increasingly more often towards the end of each ~20minute session (Figure 1 - figure supplement 4, mice). Mice tended to decrease their body movements prior to a lever pull and we did not find evidence of stereotyped behaviors prior to lever pull (Figure 1 - figure supplement 5; see also Methods section on detecting stereotyped movements). Similar to the RP in humans, self-initiated behaviors in mice are preceded by an increasingly stereotyped average widefield [Ca++] signal up to 5 seconds or earlier in several areas including motor and limb cortex (Figure 1e, Figure 1 - figure supplement 3). This common dynamical pattern was observed in all sessions and animals but not when considering random segments of neural activity (Figure 1 - figure supplement 3).

Self-initiated movements in mice can be decoded seconds prior to action from preceding neural activity. In addition to the human RP, several human fMRI studies have shown that voluntary behavior

could also be decoded up to several seconds prior to movement, usually a few percent above chance (Fig 1f,g; Soon et al 2008; 2013; Bode et al 2011). To compare with human studies, we trained support-vector-machines (SVMs) using trials within each session to decode upcoming rewarded lever pulls (Fig 1h) or spontaneous limb movements (Fig 1i,j). We decoded, i.e. classified, (i) neural activity preceding a self-initiated action (e.g. rewarded lever pull) vs (ii) neural activity representing random periods of behavior similar to two class voluntary choice decoding carried out in humans (e.g. Soon et al 2008; note: we defined random activity as continuous segments of neural data that were centered at least 3 sec outside of lever-pull times; see Methods). Within each session we used sliding windows of 1sec of neural activity as input to the SVMs. Additionally, we trained markerless pose estimation methods to track the spontaneous limb movements of mice (see Methods). To disambiguate the effects of multiple sequential lever pulls, we considered only lever pulls that were preceded by at least 15 seconds of no-lever pull activity (see further results below and Methods on lever lockout analysis). Upcoming rewarded lever pulls could be decoded several seconds prior to movement with decoding accuracy curves improving closer to the lever pull time (examples in Fig 1h).

In sum, neural activity preceding self-initiated lever pulls in mice is preceded by multi second stereotyped changes in widefield [Ca++] cortical activity similar to the human RP. Similar to human fMRI results, upcoming lever pulls or spontaneous limb movements could be decoded from preceding neural activity with similar decoding accuracy previously reported in humans (e.g. Soon et al 2008; Bode et al 2011). Our findings suggest that, like humans, mice may also engage pre-movement neural dynamics spanning several seconds prior to self-initiated action.

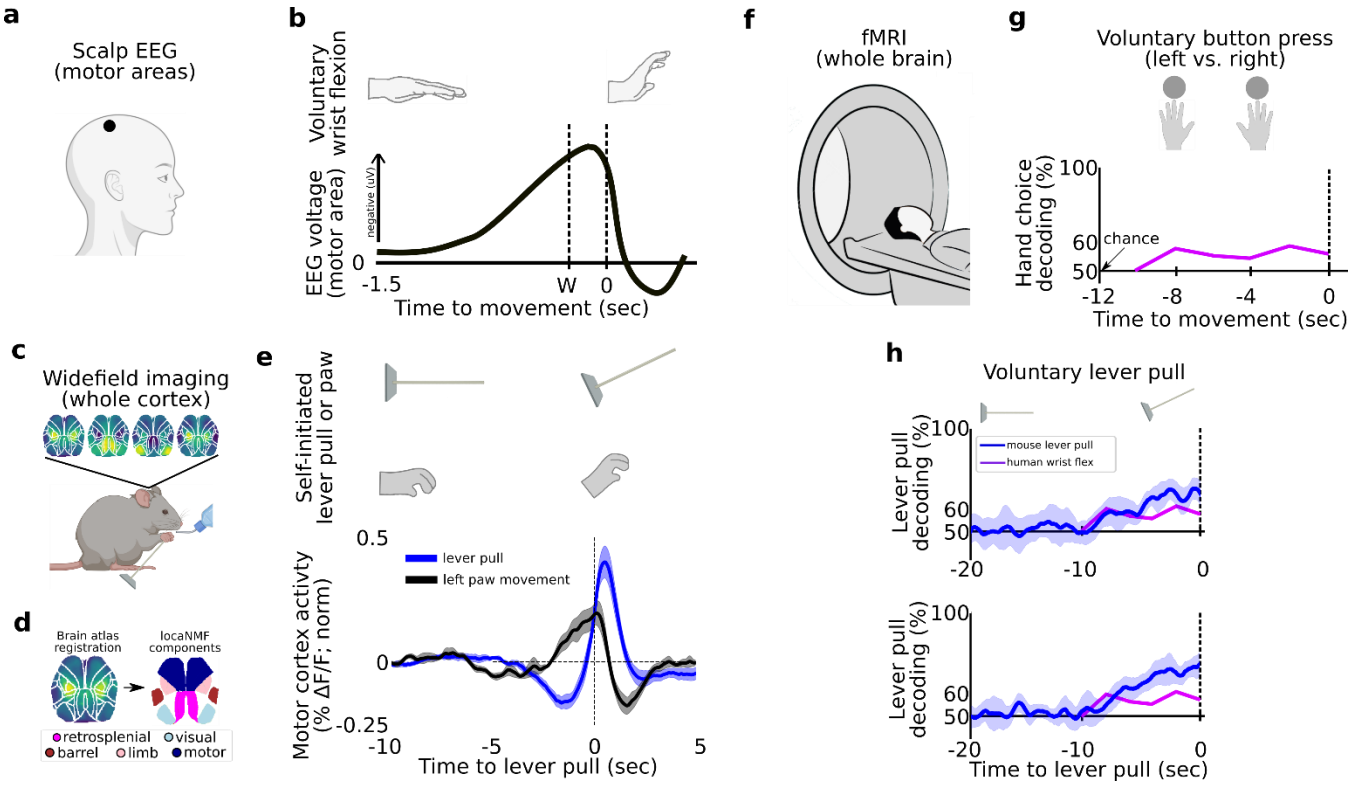

Figure 1. Detecting and decoding upcoming self-initiated mouse behaviors via widefield calcium activity. (a) Human voluntary behavior studies using scalp EEG target motor cortex and related areas. **(b)** Human voluntary wrist flexion studies recording EEG from motor areas (as in (a)) reveal a change in neural activity 0.5-1.5sec prior to behavior initiation (t=0sec) or even awareness (t=W) in some studies (note: the y axis of the plot is inverted so the RP is negative). **(c)** Mice learn to voluntarily self-initiate a lever-pull to receive water reward while widefield [Ca++] activity is captured at 30Hz. **(d)** Allen Brain Atlas and locaNMF decomposition of neural activity into neuroanatomical areas (see also Methods). **(e)** The average motor cortex widefield calcium (neural) activity (solid blue line) becomes increasingly stereotyped prior to a self-initiated lever pull (t=0sec; data shown is from 21 sec locked out trials; dashed line represents Hilbert transform of oscillatory signal). **(f)** Human studies seeking to decode voluntary choice relying on fMRI imaging during voluntary behaviors. **(g)** Decoding accuracy for left vs. right hand voluntary button presses (solid purple line) is a few percent above chance several seconds prior to movement initiation and peaks at approximately 10% above chance at movement time. **(h)** Two

examples of decoding accuracy for rewarded lever pull vs. random states in mice (solid blue lines; shading is the standard deviation of 10 fold cross-validation accuracy) showing increases seconds prior to movement and peaking > 30% above chance at movement time (data shown for two examples of long EDTs obtained from mice M2 and M3 using 15 sec locked out low-pass filtered trials; see main text). Figure 1 b has been adapted from Box 1 in Haggard 2008. Figure 1 g has been adapted from Figure 2 in Soon et al 2008.

Fig 2. A cortex wide distributed multi-second neural code underlies self-initiated actions

Figure 2 Here

We sought to systematically evaluate decoding accuracy for upcoming behaviors across mice, by evaluating multiple cortical anatomical areas and for different movements (e.g. water rewarded lever pulls or spontaneous limb movements; Fig 2).

Decoding future rewarded lever pulls seconds prior to movement. We next focused on decoding water rewarded lever pulls: i.e. lever pulls that reached a minimum lever angle and were not preceded by a previous lever pull for at least 3sec (Fig 2a; Sup Fig 2.1; see also Fig 4 and Methods). Going back in time from t=0sec, we defined the earliest-decoding-time (EDT) as the last point in time at which the SVM accuracy was statistically higher than chance (Fig 2b, 10 fold cross-validation pval < 0.05, student 1 sample t-test corrected for multiple hypotheses using the Benjamini-Hochberg method; see Methods). The decoding accuracy was better than chance seconds prior to movement and gradually increased closer to the lever-pull (i.e. t=0 sec). EDTs ranged from 0 sec (i.e. lever pull was not predicted) to more than 13 seconds in some sessions (see Fig 2c for example EDTs). We also found a correlation between the number of trials within a session and EDT suggesting that EDTs could in principle be even lower (i.e. earlier decoding in time) than reported in our study (Fig 2c linear fit; note each EDT was computed from a single session; see also Methods). To evaluate this correlation, trials from sequential sessions were concatenated to obtain at least 200 cumulative trials resulting in improvement in EDT (Figs 2d,e). Pooled sessions EDTs were lower for all mice (Fig 2f - left panel; pvals < 0.01 for all animals; single session averages in seconds: M1: -2.91; M2: -2.87; M3: -4.75; M4: -3.55; M5: -4.32; M6: -6.91; concatenated averages in seconds: M1: -4.84; M2: -5.47; M3: -7.58; M4: -5.76; M5: -6.99; M6: -6.92).

Given the strong dependence of EDT on the # of trials, we sought to re-evaluate EDTs using only trials that were not preceded by another lever pull (either rewarded or non-rewarded). We find that oscillations observed in the neural data are likely enforced by repetitive and stereotyped recent lever

pulls and that EDT analysis requires exclusion of trial that occur too soon after a previous lever pull (here we chose a lockout of 15 seconds; note: this approach significantly decreased the number of trials available for analysis as mice only rarely went without pulling the lever for 15 seconds; we thus pooled trials from across sessions into a minimum of 50 to a maximum of 200 trial hybrid-sessions; see Methods). We found that after lockout the neural data had a single negative (i.e. inhibitory) phase preceding self-initiated rewarded lever pulls that comenced ~5 seconds prior (similar to Figure 1e; see Figure 2 - figure supplement 2). We additionally found that EDTs decoded from lockout trials were shorter (Figure 2g: average EDT in seconds: mouse 1 (M1): -1.93; M2: -3.14; M3: -2.27; M4: -1.87; M5: -1.64; M6: -2.49). However, low pass filtering the neural time series (at 0.3hz) (as a type of feature engineering based on power-analysis results in Figure 7 below) resulted in EDTs more similar to the initial results (Figure 2h; average EDTs of causal filtered neural data in seconds: M1: -3.5; M2: -4.85; M3: -6.95; M4: -4.31; M5: -3.0; M6: 3.7). The improvement in EDT was qualitatively observable in decoding accuracy curves (Fig 2i) and was present even for non-lock out trials (see Figure 2 - figure supplement 4; see also Methods).

The initial loss of EDT (without the filtering step) suggests that sequential lever pulls might have a causal role in lengthening EDTs by generating stereotyped neural time series which represents preceding - not just the current - rewarded lever pulls. However, we also found that pooling trials from sessions far apart in time (days or weeks) as required by the lockout method also shortened EDT values (i.e. closer to 0 sec; Figure 2 - figure supplement 3). This suggests that higher data variance (due to learning, [Ca] bleaching, implant degradation etc.) might also have a causal role in shortening EDTs. Overall, these findings show that self-initiated water rewarded lever pulls in mice can have neural correlates that are present up to several seconds prior to lever pull and can be decoded several seconds prior to level pulls, but that such analysis must appropriately take into account previous behaviors and the effects of data variance over longitudinal studies.

Preparation of upcoming lever pulls is widely distributed across the cortex. We next evaluated decoding of upcoming lever pulls using individual cortical areas rather than the entire dorsal cortex (Fig 2i). Anatomically-informed components were obtained using LocaNMF (Saxena et al 2020; see Methods) and EDTs were computed for bilateral activity from: retrosplenial, somatosensory-barrel, somatosensory-limb, visual and motor cortex. Somatosensory-limb cortex was generally the most informative of upcoming lever pulls (i.e. lowest mean EDTs across all mice) followed by motor cortex; visual cortex based decoding had the highest EDTs (i.e. closest to lever pull time t=0sec). More importantly, using all regions for decoding yielded lower EDTs than using somatosensory-limb cortex alone (2 sample KS test comparing limb-cortex vs. all neural regions EDTS; D-statistic for all mice: 1.0; P values: M1: 0.0; M2: 5.55e-16; M3: 2.90e-22; M4: 2.77e-19; M5:4.52e-21; M6: 2.22e-16). These findings are consistent with a single neuron study in humans that showed pooling neurons yielded increased decoding accuracy of upcoming voluntary action when compared to single neuron decoding alone (Fried et al 2011) but our results yield earlier decoding times than previously shown in humans.

EDTs of non-locked out paw movements and licking events are similar to those for lever pulls. Most human studies on self-initiated voluntary behavior employ simple behaviors such as the flexing of a finger or pressing of a button with a specific hand (e.g. Libet 1983; Soon et al 2008). Accordingly, we also sought to determine whether mouse spontaneous paw movements (not just those related to water rewarded lever pulls) could be decoded from preceding neural activity (Fig 2, figure supplement 5; see Methods for description of body movement tracking methods). Briefly, we defined a self-initiated body movement as the time when the body part increased its velocity to more than 1 x the standard deviation of all movement within the session (we also implemented a 3 sec non-movement lockout period as in human studies and as in the preceding section). SVMs were trained as for rewarded lever pull times but using the body movement initiation time (i.e. t=0). As for self-initiated lever-pulls, a strong correlation was present between the number of trials within a session and the EDT suggesting that with higher

number of body movements (e.g. longer sessions) EDTs could be even lower (Fig 2, figure supplement 5a). Across all animals, upcoming body movements could be predicted above chance a few seconds prior to movement in the vast majority of sessions and in some cases more than 10 seconds prior to movement (Fig 2l). Importantly, with a few exceptions, licking or paw movements EDT distributions were not statistically different from lever pull time ETDs, however, due to the high correlation between paw movements and licking to lever pull times - we do not view them as completely independent analyses. Importantly, as we show below (see Figure 8) when considering only body movements that are isolated from lever pulls (i.e. not preceded by a lever pull in the previous 15sec, or following 5sec) and also not preceded by other body movements for at least 5sec, we find that [ca] averages show an increase in motor cortex (and other areas) and that EDTs are near 0sec as the signal is too noisy to enable decoding (see also Methods and Discussion).

In sum, upcoming self-initiated behaviors in mice can be decoded above chance several seconds prior to movement for all animals with a strong dependence of the EDT on the number of trials present in each session. While sequential stereotyped pulls have the effect of lengthening EDTs, longitudinal changes in the neural recordings have the effect of shortening EDTs. Single anatomical area analysis revealed that somatosensory-limb cortex contained the most information about upcoming movements but that decoding information was distributed across multiple regions of cortex.

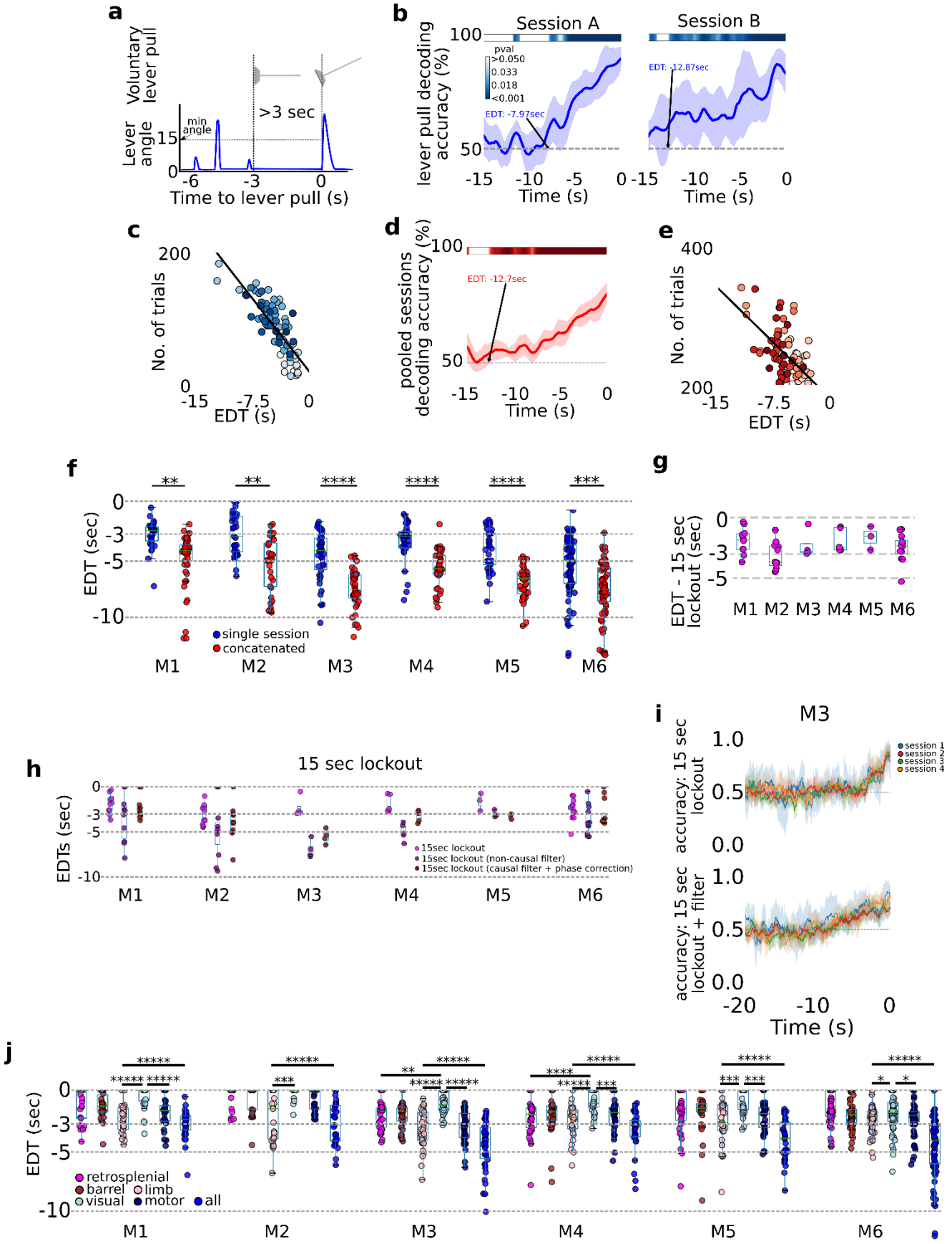
a
Voluntary lever pull
Lever angle
min angle
>3 sec
Time to lever pull (s)
b
Session A
Session B
lever pull decoding accuracy (%)
pval
>0.050
0.033
0.018
<0.001
EDT: -7.97sec
EDT: -12.87sec
Time (s)
c
No. of trials
EDT (s)
d
pooled sessions decoding accuracy (%)
EDT: -12.7sec
Time (s)
e
No. of trials
EDT (s)
f
EDT (sec)
single session
concatenated
M1
M2
M3
M4
M5
M6
g
EDT - 15 sec lockout (sec)
M1 M2 M3 M4 M5 M6
h
15 sec lockout
EDTs (sec)
15sec lockout
15sec lockout (non-causal filter)
15sec lockout (causal filter + phase correction)
M1
M2
M3
M4
M5
M6
i
M3
accuracy: 15 sec lockout
accuracy: 15 sec lockout + filter
session 1
session 2
session 3
session 4
Time (s)
j
EDT (sec)
retrosplenial
barrel
limb
visual
motor
all
M1
M2
M3
M4
M5
M6

Fig 2. Decoding self-initiated lever pulls using cortical neural activity. (a). Decoding self-initiated water rewarded lever pulls using a minimum 3 sec lockout window and a minimum lever angle threshold (see also Methods). **(b)** SVM decoding accuracy curves of two different sessions (mouse M4) reveal increased decoding accuracy near lever pull time and an earliest decoding time (EDT) of several seconds (curves represent average accuracy and shaded colored regions represent standard deviation over 10-fold cross validation; top colored bars represent p values of student t-test with a Benjamini-Hockberg correction for multiple hypotheses; see Methods for more details; note sessions shown were atypical and were selected to illustrate decoding curves for early EDTs when decoding from all trials, i.e. without locking out previous lever pulls). **(c)** EDTs from all sessions (mouse M6) show a strong correlation between EDT and the number of trials within a session (lighter colors indicate earlier sessions in the experiment). **(d)** Same as (b) but for an example from concatenated, i.e. multi-session, analysis. **(e)** EDTs for concatenated sessions (M6) also show a correlation between EDT and the number of trials present in the session and the earliest decoding time (lighter shading representing earlier sessions in training). **(f)** EDT distributions across all mice for single session trials (blue) vs. multi-session trials (red) reveals a significant lengthening (i.e. further from lever pull-time) in EDTs for multi-sessions across all animals (cyan box plots show 25th percentile, median and 75th percentile; comparisons between single vs. concatenated sessions were carried out using 2-sample KS test with asterisks indicating: * <0.05; **<0.01; ***<0.001; ****<0.0001; *****<0.00001). **(g)** Same as (f) but for 15 sec lockout trials concatenated across multiple sessions. **(h)** Recomputed EDTs for filtered calcium traces. **(i)** Examples of decoding accuracy curves for 15 sec lockout trials using filtered vs. non-filtered neural time series (see also Methods).

Fig 3. Self-initiated lever pulls occur during narrowly distributed slow-oscillation phases

Figure 3 Here

Studies of human voluntary behavior have shown that slow-cortical potentials (SCPs), i.e. slowly changing voltages measured usually via EEG < 1Hz, might be involved in modulating voluntary behavior (Jo et al 2013; Schmidt et al 2016). In particular, voluntary behavior was found more likely to occur (on the order of ~10%) when the SCP phase over motor areas was near the crest. Additionally, there is some evidence to support that the SCP is related to awareness or consciousness and may play a causal role in internal state driven action (He and Raichle 2009; Northoff G. 2007). Given these findings we sought to determine whether self-initiated lever-pulls in mice co-occurred with specific phases of widefield [Ca++] activity (Fig 3).

Lever pulls occur during narrowly distributed phases of neural activity. As shown above (see Fig 1, Sup Fig 1.3) within single cortical areas, the neural dynamics preceding rewarded lever pulls become increasingly stereotyped closer to t=0sec (Fig 3a-top for an example of left forelimb neural activity). Fitting sinusoids to the last 5sec period prior to movement in each trial yielded sinusoidal fits with very similar phases at t=0sec (Fig 3a-bottom). Neither of these stereotyped dynamics were present in random segments on neural activity (Figure 3 - figure supplement 1). The phase distribution for a single session and cortical area was narrowly distributed with most phases falling in a < 90^0 wide window in many sessions (and < 45^0 for some sessions) (see Fig 3b for example distribution from phases in Fig 3a; see also Figure 3 - figure supplement 2 for examples from all cortical areas). In contrast, random segments of neural activity had widely distributed phases (Figure 3c, Figure 3 - figure supplement 2). Computing the t=0sec phases for all trials across all sessions also revealed narrowly distributed phases (Fig 3d) in contrast to random segments of neural activity which yielded an approximately uniform distribution (Fig 3e). Similar human studies where the most likely SCP phase during voluntary action was the crest phase with ~30% probability followed by the rising phase (Fig 3f

for an adapted example), phases in mice were also biased to these two locations (i.e. crest or rising phase). In contrast to human results, we found an even higher bias as some mice had more than a 50% probability of initiating action in the crest phase - while others preferred the rising phase (See Fig 3g for 2 examples). The phases for all mice, sessions and trials showed that virtually all mice and cortical areas had narrowly distributed phases (Fig 3h) significantly different than random segments of neural activity (Fig 3i; Rayleigh test for uniformity $<<1E^{-5}$ for all animals and areas). The diversity of phase preferences was present not only between mice but also within mice as the phase bias could be significantly different between cortical areas (for example, Fig 3h, mouse M1 limb vs motor cortex phase differences). Lastly, the median inter-area phase correlation varied with some mice having highly correlated phases across areas whereas others having mostly low correlations (Fig 3j; see also Methods).

In sum, the phases of neural activity at lever pull initiation from all areas were significantly stereotyped, consistent with human findings (Jo et al 2013; Schmidt et al 2016). In contrast to human findings we found a higher bias of phases: i.e. behaviors were even more likely to occur during a specific phase in mice than in humans. These findings support the presence of biases in neuroanatomical dynamics preceding self-initiated behavior preparation while confirming inter-animal differences in both anatomy and dynamics observed in other findings (see also Figs 4, 5).

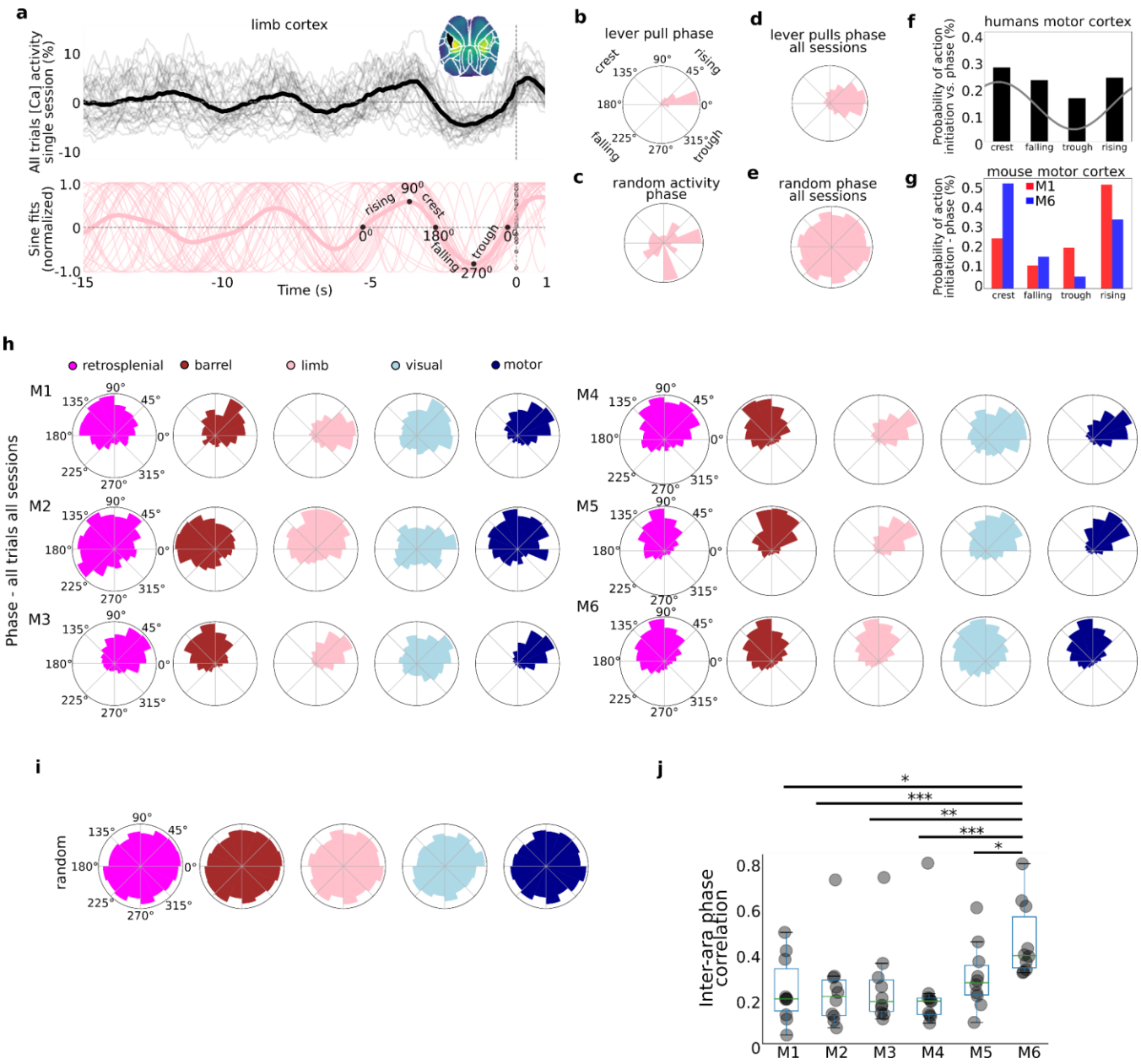

Fig 3. Self-initiated behaviors occur during specific phases of slow-oscillations. (a) Top: single trial neural activity (gray curves) from 33 trials in a single session (M4) for somatosensory-upper left limb cortex contain oscillations that become increasingly stereotyped closer to lever pull time (t = 0 sec; thick black curve is session average; inset shows anatomical area selected); Bottom: single trial sinusoidal fits (thin pink curves) to neural activity (in Top) and phases (scatter dots on the t=0 sec line; thick pink curve is session average). **(b)** Polar plot of results in (a) showing the distribution of sinusoidal fit phases

at t=0sec. **(c)** Same as (b) but for random periods of neural activity (i.e. not locked to any behavior). **(d)** Same as (b) but for all sessions in mouse M4. **(e)** Same as (d) but for random periods of neural activity across all sessions in mouse M4. **(f)** Probability of voluntary action in humans during various phases of the SCP. **(g)** Same as (f) but widefield [Ca++] from the motor cortex in mice M1 and M6. **(h)** Phase distributions across all mice, sessions and areas. **(i)** SCP phase distributions for random segments of neural activity for all areas in mouse M4. **(j)** Single trial pairwise correlation between all cortical areas (e.g. limb vs. motor, limb vs. retrosplenial etc.). Figure 3 f has been adapted from Figure 2 from Schmidt et a. 2016.

Fig 4. Changes in decoding and neural dynamics over weeks of task performance

Fig 4 here

We next sought to determine whether learning or mere longitudinal performance of the task changed the decoding accuracy or cortical neural dynamics during voluntary behavior initiations (Fig 4).

Longitudinal cortical network dynamics support shortening of EDTs. Considering the number of rewarded lever pulls per session, we found that between the first and last days of the experiment three of the mice (M2,M3 and M6) increased the number of rewarded lever pulls while one additional mouse (M5) also had a positive trend (with pval of 0.13); one of the mice (M1) decreased its number of pulls per day and the remaining mouse did not have statistically significant changes (Fig 4a; pearson correlation values provided in figure insets; see Methods). We labeled the 4 mice with either a strong or a trend in positive correlation over time as the "performer" group (M2, M3, M5 and M6) and the remaining mice (M1, M2) as "non-performers" as they did not increase their pulls over time. Given the potential confounds identified in Fig 2 between sequential lever pulls and decoding time, further analysis in this section focused primarily on 15 sec lockout trials only (see Fig 2). We found that SVM decoding accuracy curves over the weeks or months of behavior revealed potential trends over time (Fig 4b for examples from 2 mice). In particular, we found that EDTs shortened (i.e. were closer to the lever pull time) over time in 2 mice (M1 and M6); a similar trend was present in another mouse (M5; pval 0.06); while the remaining three mice did not show statistically significant trends. Although only statistically significant in two mice, shortening of EDT decoding time trends may be explained by automaticity findings in other studies: i.e. that following learning and repetitive behavior performance, the control of behavior is transferred from cortical structures (which we had access to during widefield [ca] imaging) to subcortical structures (that we could not access in our paradigm; another explanation could be that implants slowly degraded) (see e.g. Ashby et al 2010; see also Discussion).

Lever-pull neural activity space increases its cortical representation over time in some mice. We implemented a convex-hull based analysis to capture how the neural activity *space* prior to lever pulls changed over weeks or months of performance (Figs 4d-g; see Methods). For each session, the neural activity *convex hull* at lever pull time (i.e. t=0 sec) was defined as the hyper-volume that enclosed the t=0 sec neural activity vectors relative to all the neural activity vectors in the session (note: as convex hull analysis is sensitive to outliers a 10% K-nearest-neighbor triage was implemented prior to evaluation; see Methods). The convex hull could be visualized in two dimensions using PCA as the area enclosing the t=0sec neural activity vectors for lever pulls in that session (Fig 4d-blue dots; see also Methods). Both the convex hull of the t=0sec and t=-1sec period prior to lever pull occupied a small subspace within the entire neural space of all the activity in the session (Fig 4d-colored dots; see Methods). Going backwards in time, the convex hull space gradually increased further away from t=0sec (Fig 4e). This suggests that neural activity looks more like spontaneous (i.e. random) activity further in time from lever pulls and becomes more stereotyped towards t=0sec. The ratio of the pre-pull convex hull to the hull of the entire session was smaller than the hull computed from random trigger times (Fig 4f).

Lastly, we evaluated the area under the ratio curve (AUC) longitudinally to evaluate whether there are systematic changes in the neural activity convex hull over weeks of behavior performance (Fig 4g). We carried out this analysis using only 15 sec lockout data grouped in sessions of up to 200 trials (similar to carried out above to exclude any possible trends arising from increased intra-session lever pulls or effects of sequential lever pulls; see Methods). We found that, as in the EDT longitudinal trends, 2 mice (M1, M6) that had decreasing EDTs (i.e. poorer decoding over time) also had an increased similarity (i.e. increased AUC values) between lever pull dynamics and random neural states. Considering only these two mice (as they were the only statistically significant results), one explanation may be that cortical dynamics may return to pre-lever pull learning patterns and look increasingly the

same as random neural states (occurring near or far from behaviors) because subcortical circuits increasingly facilitate and "take over" self-initiated behavior preparation during automaticity processes.

Neural activity space of right paw movements and lever-pulls change systematically over time in some mice. Given the findings above we sought to further evaluate systematic changes between lever-pull and random neural activity (Fig 4h-j). We recomputed convex hulls for the 1sec period prior to lever-pull, 1sec period prior to left paw and right paw movements and found that the size of the lever pull convex hulls and its overlap with the rest of the behaviors changed over time (Fig 4h). While 5 of the 6 mice had increasing convex hulls, the trends were statistically significant in only 2 of the mice, which again, were mice M1 and M6 (although mouse M3 also showed a similar trend, p value: 0.14) (Fig 4i). Interestingly, mouse M4 showed a decrease in overlap of lever dynamics with all dynamics. These mixed results suggest that different mouse-specific mesoscale neural representations may be involved during learning and performing of a task.

We also found mixed results with respect to the <u>intersection</u> between the <u>right paw</u> convex hull, i.e. the paw used to pull the lever, and the <u>lever pull</u> convex hulls: the overlap decreased with time in 2 of the mice (M4 and M6) and showed a similar trend in another mouse (M3; pval 0.09); and it increased with time in mouse M1. These results suggest that in some mice (M4, M6 and possibly M3) lever pull neural dynamics increasingly specialize or differentiate from non-lever pull right paw movements neural dynamics (despite the right paw being used for the lever pull task). In contrast, in one mouse the similarity between right paw movements and lever pulls increased (e.g. mouse M1), but this could be explained by this mouse being a behavior outlier as the only mouse with decreased number of rewarded lever pulls over time..

In sum, EDTs shortened longitudinally in some mice suggesting neural dynamics underlying self-initiated behavior might be transferred from cortical to subcortical circuits decreasing the power of cortical-based decoding methods. The convex hull of the neural activity prior to self-initiated lever pulls

also increased over time in some mice with a potential explanation that cortical dynamics return to pre-learning similarity over time. Lastly, right paw and lever dynamics appeared to become increasingly dissimilar in a few mice, with one mouse showing the opposite trend. These findings suggest that learning or mere longitudinal performance of a task restructures the neural dynamics underlying self-initiated action but that the effects could be subject specific, drawing attention to the need for intra-animal analyses (rather than cohort) in future studies.

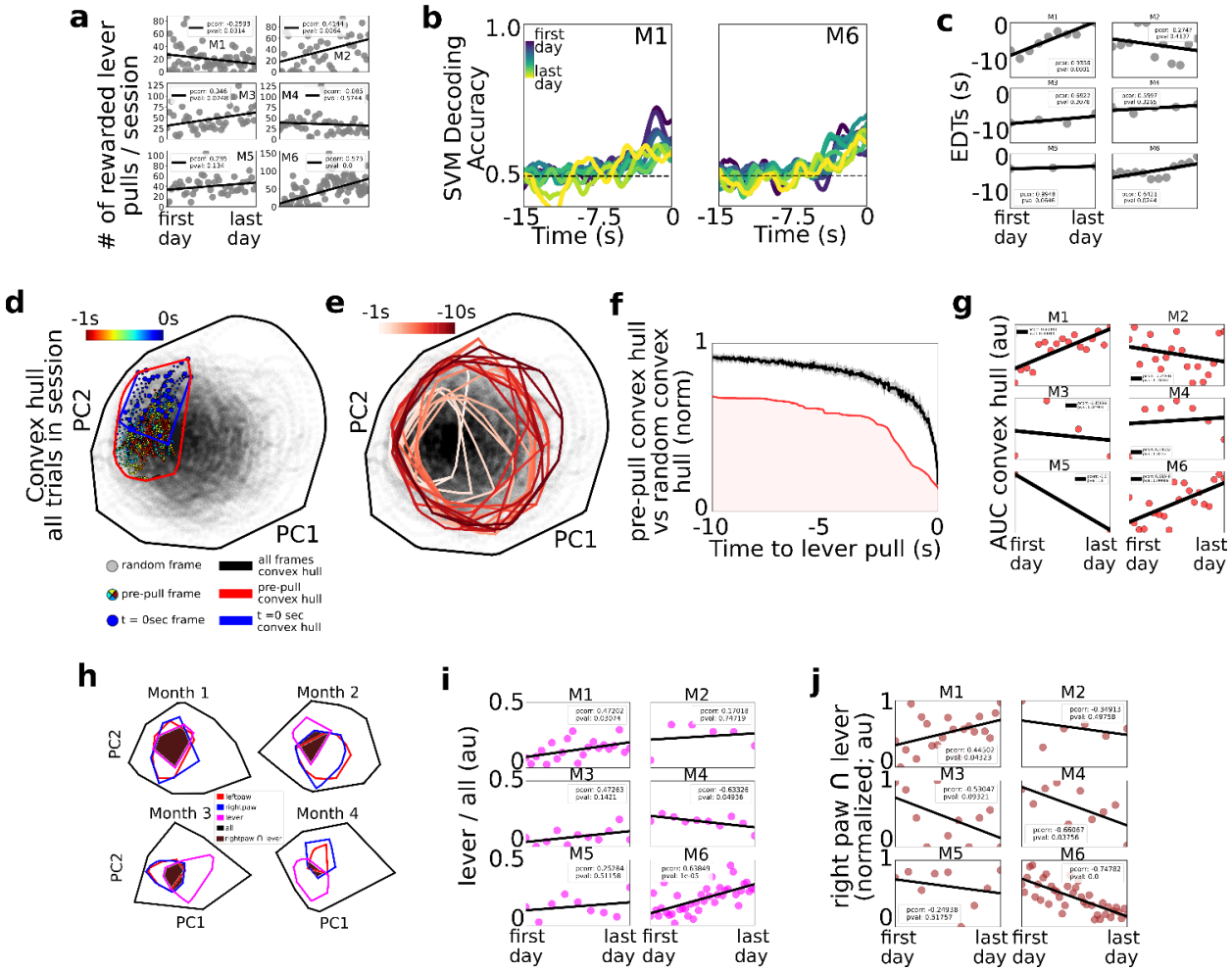

Figure 4. Tracking changes in decoding performance and spontaneous neural dynamics over time. **(a)** Number of rewarded lever pulls per session in all mice over the duration of the experiment. **(b)** SVM decoding accuracy curves from M1 and M2. **(c)** EDTs (black dots) for all mice (using 15 sec lockout trials only (black lines: linear fits; inset: pearson correlation coefficient; note: the EDTs were computed on non-lockout data). **(d)** Convex hull of neural activity preceding lever-pulls from 30 trials from a single session in mouse M3. The colored scatter points represent neural activity at various frames in the -1sec to 0sec period and the polygons represent the convex hull of neural activity for all data (black), t = 0 sec (blue) and t= -1sec to t = 0sec (red; see also legend for details). **(e)** Same as (d) but for 1sec segments ranging from -10sec to t = 0 sec. **(f)** Convex hull volume (red line; shading represents AUC) of pre-pulls vs. random segments (black line; shading represents 10-fold sampling standard deviation; see

also Methods). **(g)** AUC (scatter points) of ratio curves (as in (f)) for all animals and sessions. **(h)** Convex hull of 1sec of neural activity preceding body movements (red and blue polygons), lever pull (magenta polygons) and all neural data (black polygons) at different longitudinal time points in the experiment for mouse M6. Brown shaded regions represent the overlap between the right paw movement initiations and lever pull. **(i)** Ratio of convex hull of lever-pull to all neural activity (magenta scatter points), linear fit (black line) and pearson correlation value (inset). **(j)** Intersection of right paw and lever pull initiation space (brown scatter points), linear fit (black lines) and pearson correlation (inset).

Fig 5. Single trial variance changes seconds prior to self-initiated lever pulls

Figure 5 here

Over the past few decades one of the most robust findings in stimulus cued decision making studies has been that stimulus onset decreases neural variability in a wide range of paradigms (see Churchland, Yu et al 2010 for a summary). This decrease in variance, also evaluated as the fano factor (i.e. the ratio of variance to mean of neural activity) has been interpreted to suggest that incoming information (i.e. stimuli) "stabilizes" the state of cortical activity (e.g. decreases the variance of membrane potential fluctuations, spiking variance or correlated spiking variability) and potentially supports the accumulation of internal memory evidence (Ratcliff 1978; Ratcliff and McKoon 2008). Here, we sought to determine whether neural activity preceding self-initiated lever-pulls exhibited a change in variance prior to the decision to pull, potentially reflecting the commencement of evaluation of "internal-state" evidence and/or the preparation of a skilled action (Fig 5).

Single trial variance decreases seconds prior to self-initiated action. As shown above for single trials (Fig 3a), the average trial activity within a session becomes increasingly stereotyped near t=0sec. This stereotypy can be observed in all major cortical areas even across weeks or months of behavior (Fig 5a). Interestingly, the variance was also stereotyped with a significant change (decrease in 5 mice; increase in 1 mouse: M2) several seconds prior to the movement related areas (e.g. motor, somatosensory and retrosplenial) but less so in areas not directly related to movement preparation (e.g. visual cortex; Fig 5b). We defined the earliest-variance-decrease-time (EVDT; see Methods) for each session as the time at which the variance decreased (or increased for mouse M2) by two times the standard deviation from a random period of time (Fig 5b - black dots; see Methods). Computing the EVDTs for all sessions and mice revealed that in most areas and animals the neural activity variance began to decrease a few to several seconds prior to lever pull initiation. While these measurements were noisy (see Methods), in mice with significant numbers of detected EVDTs (i.e. mice M3, M4, M5 and

M6) the average EVDT for all areas was around -3sec or earlier. Such decreases in variance seconds prior to behavior initiation may represent the times at which internal state evaluations and motor preparation commences (see also Discussion; we note that this analysis was not possible using lock-out trials due to significantly higher intra-session variance caused by pooling data from across sessions days and weeks apart; given EDTs ranging from approximately -3sec to -7 sec for lockout data we anticipate that given sufficient numbers of 15sec lockout trials we would obtain similar or shorter EVDT times as in non lockout data).

In sum, we found that in most mice and sessions, variance across all areas (excluding visual cortex) began to change several seconds prior to lever pull time. These results are consistent with and support our prior findings and could be interpreted to suggest that internal-state driven behaviors are underpinned by neural processes similar to those observed in stimulus driven decision making studies (and as observed in Murakami 2014 in neural activity preceding a self-paced task).

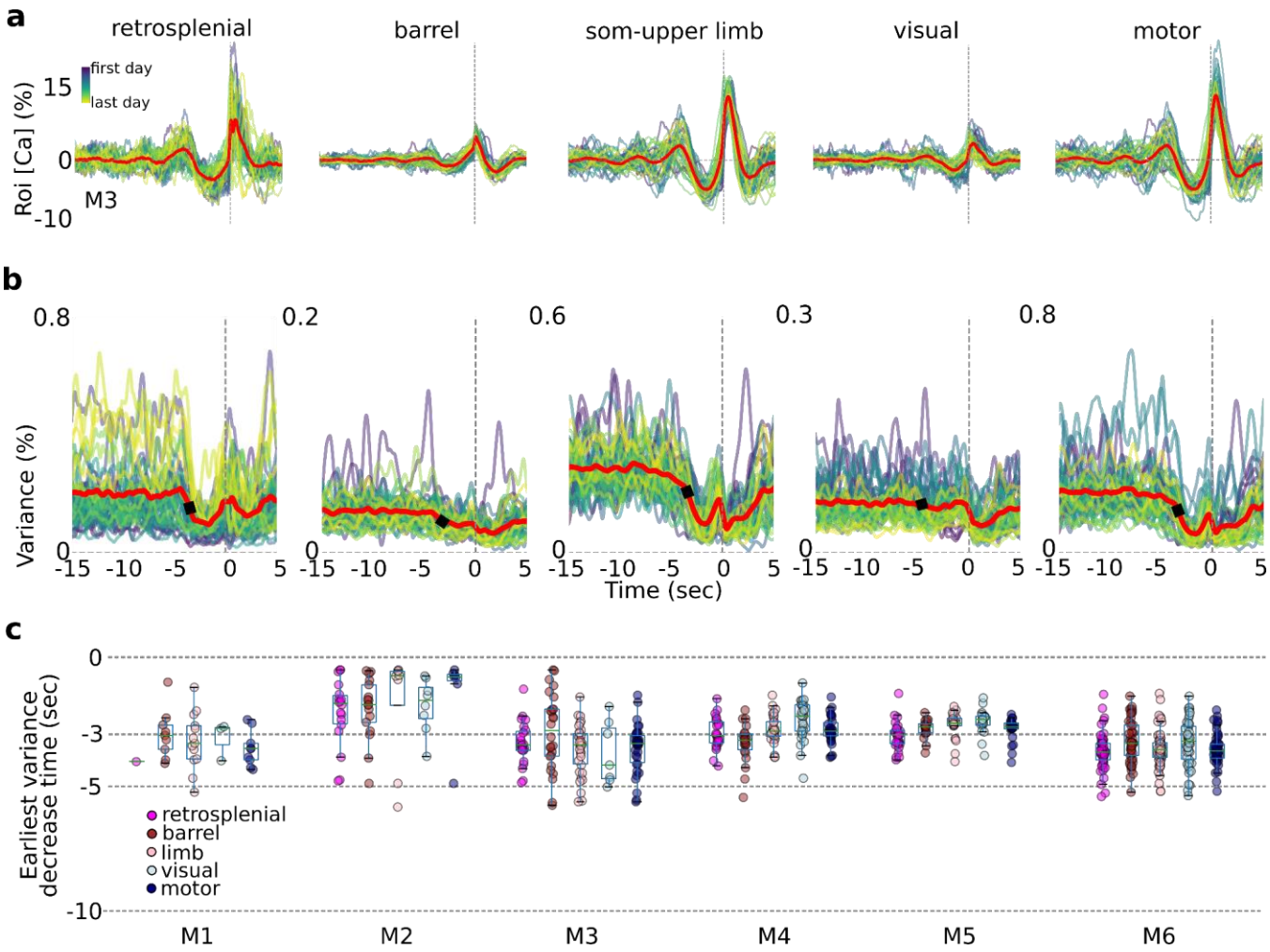

Figure 5. Internal-state evaluations begin several seconds prior to self-initiated lever pulls. (a) Average session neural activity from cortical areas (colored curves) and average over all sessions (red curve) from mouse M3. **(b)** Variance of data in (A) and the earliest variance decrease time (EVDT; black dots represent EVDT of all session averages, i.e. red curves in (a)). **(c)** EVDTs for all animals and sessions.

Fig 6. Evaluation of pre-ever pull movements and behavior lockout on EDTs

Fig 6 here

An outstanding question in voluntary behavior neuroethology is how confounds, such as random body movements occurring in the period prior to a targeted action, affect behavior preparation and - in our paradigm - the decoding of future behaviors. For example, in animals that perseverate and pull the lever frequently it is not known whether decoding methods leverage dynamics from multiple lever pulls or just the lever pull occurring at t=0sec. Accordingly, we sought to evaluate the effect of preceding lever pulls and/or body movements on the decoding of future lever pulls.

Rewarded lever pulls form a small portion of all self-initiated actions. Across the duration of the study mice performed between 1454 (M1) to 6999 rewarded lever pulls (M6) (Fig 6a). The ratio of self-initiated rewarded and non-rewarded lever pulls, licking events, and left paw and right paw spontaneous movements for all sessions revealed that lever pulls constituted only a small portion of behaviors (Fig 6b). Across all animals the proportion of rewarded lever pulls compared to all other movements ranged from 0.03 (M1) to 0.07 (M2) (Fig 6c). Even though only selected body parts were tracked (i.e. paws and tongue), these results suggest the vast majority of the time mice are engaging in carrying out many other spontaneous behaviors as reported in other studies (e.g. Musall et al 2019).

Removing pre-action confounds by implementing a post-hoc lockout period. To evaluate the effect of intervening body movements in decoding future actions, we evaluated decoding upcoming rewarded lever pulls or spontaneous body movements preceded by periods of quiescence of varying durations (Fig 6d-h). All trials across all sessions were pooled (similar to the concatenated analysis in Fig2) and decoding was carried out after "locking-out" previous (i) lever pulls (i.e. rewarded and non-rewarded), (ii) licking events or (iii) left paw movements (note: we selected left paw movements as the right paw was used to pull the lever and excluding such movements from analysis would remove most of the rewarded lever pull trials). The number of rewarded lever pulls preceded by periods of non-body

movements or lever pulls decreased approximately exponentially with increasing lockout duration (Fig 6d). This decrease in available trials for analysis was present in all mice (Fig 6e). Importantly, locking out licking and lever paw movements beyond three seconds yielded insufficient numbers of trials for decoding analysis (see shaded region Fig 6e).

Lever pull EDTs are not affected by prior licking events. EDTs were recomputed by locking out (i.e. removing) lever pulls that were preceded by licking events in the previous 0sec, 1sec, 2sec and 3sec (note: 0sec bin removed lever pull trials that occurred exactly with a licking event based on our video recording resolution of 15FPS). We found that for all animals, the intra animal EDT distributions were not statistically different from each other (Fig 6f).

Evaluating lever pull EDTs versus lever-pull lockout duration. We also recomputed EDTs for each animal and session after enforcing periods of 3-15sec of lockout (in increments of 3sec) (Fig 6g). EDTs for two mice (M1 and M2) stayed the same, while for four mice they shortened with increasing lever-pull lockout duration (M3-M6) (Fig 6g). This trend was confirmed by examining the mean EDT at each lockout time point which showed in nearly all mice (excluding M2) a strong trend for the mean EDT to shorten with increasing lockout (Fig 6h). In interpreting these results it is important to note that there were substantially fewer consecutive or same-session lever pull trials when implementing increasingly longer lockouts. Thus, surviving trials used for analysis came from sessions that were increasingly further apart (e.g. multiple days or even a week). Pooling trials from separate days or weeks provides an additional source of noise due to changes in animal behavior, [Ca++] indicator properties, and longitudinal network changes observed in our cohorts (see Fig 4). As evidence for this, we found that subsampling the number of non-lockout trials to match the number of trials following 15sec lockout had the effect of shortening most EDTs (Figure 2 - figure supplement 3).

We also recomputed locked-out EDTs for each animal (as in (g)) but following low-pass filtering the neural time series (filter set to 0.3Hz; see Methods) as described above (Fig 6i). We found that

average EDTs detected were longer than using non-filtered data (Fig 6j; e.g, 15 sec lock out data means: M1: -3.50; M2: -4.85; M3: -6.95; M4: -5.01; M5: -3.0-; M6: -3.70).

Taken all these factors into account, the results suggest that while EDTs shortened when using only lockout trials, the cause of the increase is due to: (i) removing stereotyped sequential lever pulls which could artificially bias the neural signal; and (ii) increased variance in the longitudinal data caused by [Ca++] state changes, systematic neural network restructuring due to longitudinal performance and other unknown factors (see also Discussion).

In sum, we find that despite carrying out thousands of rewarded lever pulls, such pulls constituted a small percentage of overall spontaneous body movements (likely much less if we consider other body movements we did not track). Even when pooling all trials from each animal (resulting in thousands of trials), when locking out previous licking events or left paw movements, exponentially fewer rewarded lever pulls were available with increasing locking out period. EDTs computed when excluding previous lever pulls for a period of up to 15 seconds prior shortened EDTs in most animals, and average EDTs for band-passed neural data ranged from approximately -3sec to -7sec. We conclude that it is <u>critical to exclude sequential lever pulls to the computation of EDT</u> as well as track and control for longitudinal changes in neural dynamics caused by learning or implant related causes.

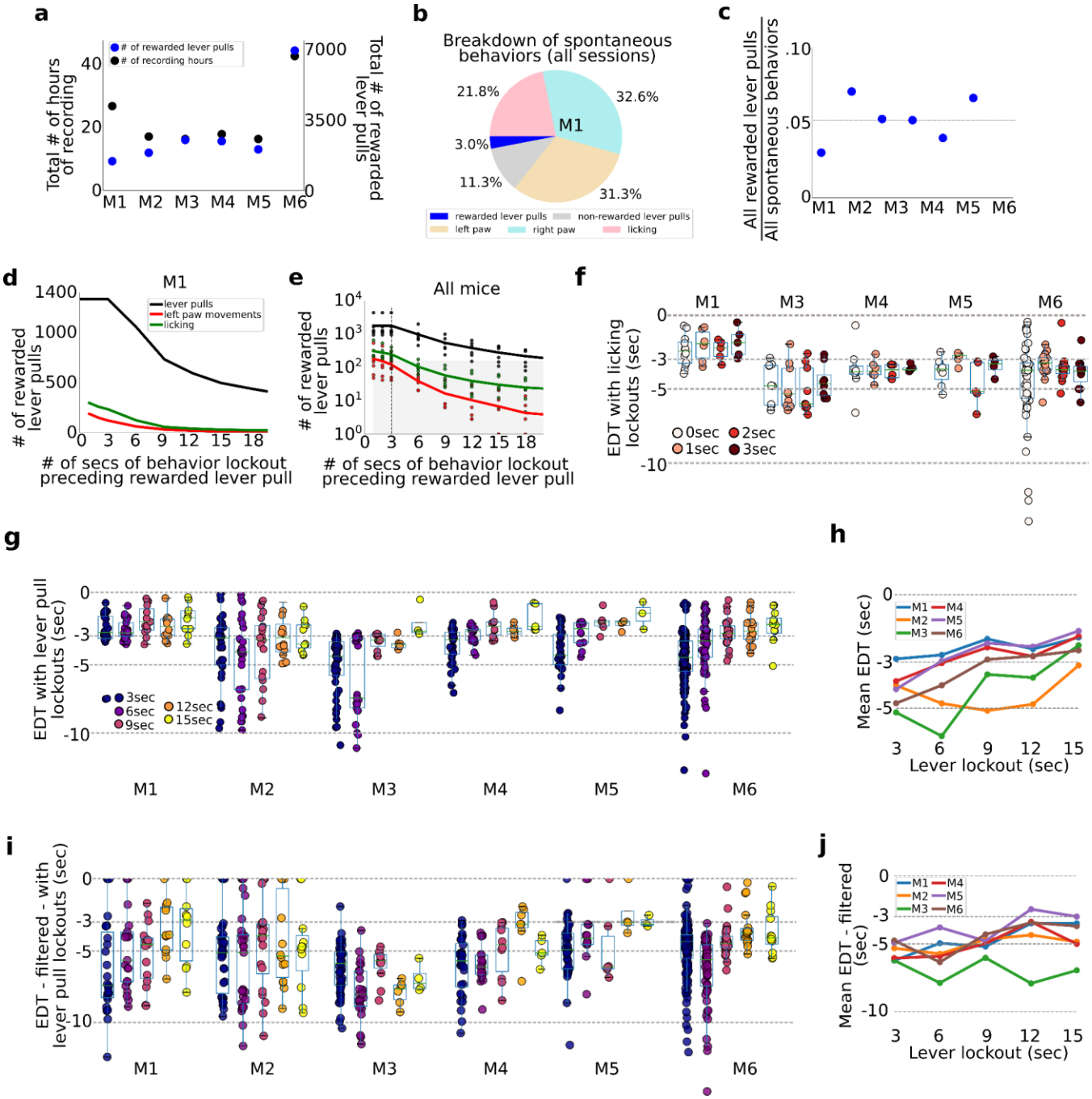

Figure 6. Tracking and evaluating the effects of previous self-initiated movements on the decoding of rewarded lever pulls. (a) Total number of recording hours and number of lever pulls for each mouse (note each recording session was approx. 22 minutes long). (b) Percentage of rewarded lever pulls, non-rewarded lever pulls, and left paw, right paw and licking movements performed by mouse M1 across all sessions. **(c)** Proportion of rewarded lever pulls relative to all other body movements for all animals. **(d)**

Number of rewarded lever pulls as a function of “locking out” previous lever pulls, licking events or left paw movements (note: locking out means excluding any rewarded lever pull trial that was preceded by a movement in the previous n-seconds; see also Main text and Methods). **(e)** Same as (d) but for all animals and sessions (shaded region indicates lockout conditions under which less than 100 trials were present across the entire study and decoding was not carried out). **(f)** EDTs for rewarded lever pulls conditioned on licking event locking out periods of 0sec - 3sec (for clarity, the 0sec time point excluded any rewarded lever pull that occurred precisely at the same time as a licking event, i.e. to the resolution of our 15FPS video). **(g)** Same as (f) but conditioned on excluding previous lever pulls (3sec time point excluded any rewarded lever pulls that occurred exactly 3sec after a previous rewarded or unrewarded lever pull). **(h)** Mean EDTs from (g) as a function of lever pull lockout period. (i) Same as (g) but following low pass filtering of the locaNMF components. (j) same as (h) but for data in panel (g).

Fig 7. Slow oscillations dominate pre-self-initiated behavior neural dynamics

Figure 7 here

While the role of SCP in modulating voluntary behavior is suggested in some human studies (Schmidt et al 2016), less is known about the specific frequencies involved in self-initiated action especially in mice. We thus sought to further characterize the frequency, power and longitudinal characteristics of slow oscillations in neural activity occurring prior to lever pulls (Fig 7).

Limb and motor cortex oscillations have the highest power during pre-movement neural activity. We first evaluated the power of neural activity in a session (i.e. average of neural data from all trials from -15sec to 0sec) and observed that high amplitude oscillations were present in some areas (e.g. limb cortex) but were much weaker in other areas (e.g. visual cortex) (Fig 7a). This is consistent with our self-initiated behavior task as no sensory stimuli or cues were used. This difference was consistent across all sessions with limb cortex oscillations being up to 10 times larger than those in visual cortex (Fig 7b examples from mouse M4).

Frequency and power in the average pre-movement neural activity. We evaluated the peak frequency of session averages (i.e. we computed the power-spectrum-density of the lever-pull trial average for each session; ses also Methods). Across all mice the vast majority of session averages had power peaks falling between 0.2Hz and 0.6Hz (Fig 7c). This suggests that slow oscillations dominated the pre-movement neural activity consistent with our findings that self-initiated action preparation unfolds on time scales of several seconds (and consistent with the time course of our [Ca++] indicator). Turning to longitudinal trends, few statistically significant trends were present with only 3 mice showing correlations of peak frequency and time (Fig 7c; mouse M1: strong increase in peak frequencies in limb and motor cortex; mouse M2: strong decrease in peak frequencies in limb and motor cortex; and mouse M5 had an increase in peak frequency in retrosplenial cortex). The peak frequency power also exhibited differences between animals and also longitudinally (Fig 7d). For example, mouse M1 showed

significant drops in power in limb, motor and retrosplenial cortex, while other mice showed increases in power in limb or motor cortex (M2: limb; M3: motor; M4: motor; M6: limb). In sum, longitudinal changes in peak frequencies and power were minor and differed across animals.

Frequency power in single-trial pre-movement neural activity. We carried out a similar analysis as above but on an individual trial basis (Fig 7e,f). With respect to peak frequencies, distributions of frequencies from ~0.1Hz to ~0.5Hz were observed, similar to session averages. In contrast with session averages, single trial analysis showed more statistically significant trends (p values < 0.05) in most animals and areas considered (retrosplenial, limb and motor cortex): three animals had mid to strong-level increases in peak frequency (in all areas) with time (M1, M4 and M5); one animal (M6) had slight increases in frequency power in retrosplenial and limb cortex; and 1 animal has mid to strong decreases in peak frequency over time (M2) (mouse M3 had a -0.01 pearson correlation value with time in limb cortex). Peak power trends were less common, with only 2 mice showing strong correlations in the three areas longitudinally (M1 decreases in power over time; M4 increases in power over time) with the remaining mice having changes only in a single area (mouse M2 showed strong decrease in power in limb cortex; and mice M3 and M6 showed a slight increase in motor cortex power over time).

In sum, during self-initiated behavior preparation power in both session averages and individual trials was strongest in the 0.1Hz-0.7Hz. Some animals showed systematic changes in peak frequency suggesting that learning and/or longitudinal performance may change the underlying oscillatory structure of neural activity of self-initiated behavior preparation. These findings suggest a complex picture with different mice potentially engaging different learning mechanisms and areas that should be considered when evaluating in-session and longitudinal performance and decoding upcoming behaviors.

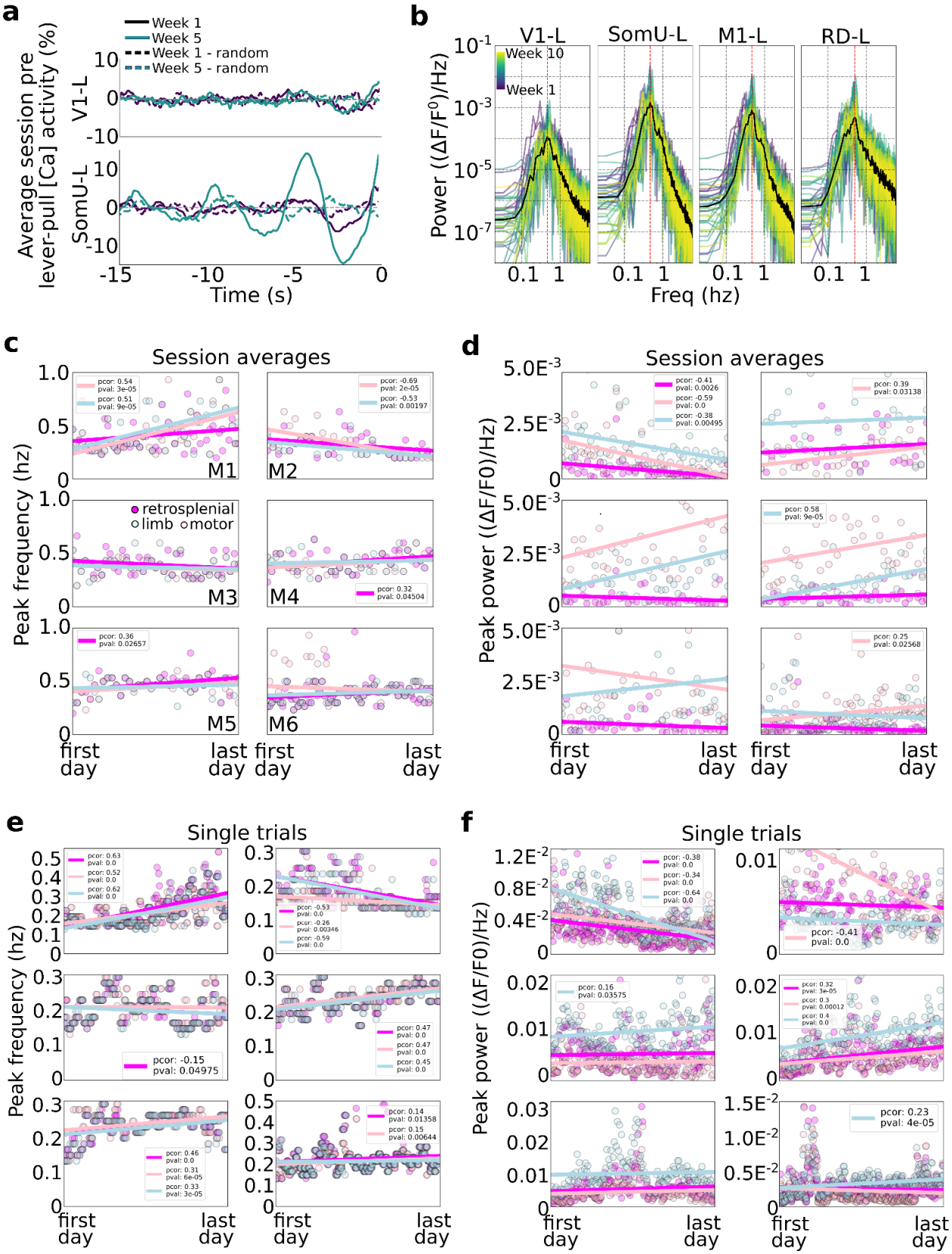
a
Week 1
Week 5
Week 1 - random
Week 5 - random
Average session pre lever-pull [Ca] activity (%)
V1-L
SomU-L
Time (s)
b
V1-L
SomU-L
M1-L
RD-L
Week 10
Week 1
Power ((ΔF/F0)/Hz)
Freq (hz)
c
Session averages
Peak frequency (hz)
retrosplenial
limb
motor
M1
M2
M3
M4
M5
M6
first day
last day
d
Session averages
Peak power ((ΔF/F0)/Hz)
e
Single trials
Peak frequency (hz)
f
Single trials
Peak power ((ΔF/F0)/Hz)

Fig 7. Slow wave oscillations underlie self-initiated behavior in mice. **(a)** Examples of single session averages (dark continuous curves) from two time-points and random segments (dark dashed curves) from V1-left and somatosensory-upper limb left reveal the presence of oscillations. **(b)** Power spectra of all session averages (colored curves) and average across all sessions (black curves) from mouse M4 in four cortical areas (dashed vertical lines indicate peak of average). **(c)** Peak frequency power of each session trial average for retrosplenial, motor and limb cortex (colored scatter points). **(d)** Same as plot in (c) but for peak power for all animals and sessions. **(e)** Same peak frequency analysis as in (c) but for single lever pull trials (instead of session averages). **(f)** Same peak power analysis as in (d) for single trials.

Fig 8. The widefield [ca] activity correlates of self-initiated limb movement vs. goal-oriented actions.

Figure 8 here

Given the results in Figures 1 - 7, namely, that prior to rewarded lever pulls there are systematic changes in cortex, e.g. inhibition of motor activity, on the order of several seconds prior to movement we sought to relate our results to human EEG studies of volitional action. In human volitional studies the motor cortex EEG signal preceding spontaneous body movements (e.g. flicking a wrist, pressing a button) generally shows an increase in activity commencing between -2sec to -1sec prior to the body movement. To compare our results to human studies we evaluated the [ca] activity preceding isolated random left forelimb movements, i.e. movements that were not related to lever pulls nor preceded by other movements for several seconds.

Identifying left paw movements isolated from other movements. We first computed the locations of all lever pulls relative to every left paw movement in windows of 20sec with 15sec of pre-paw movement and 5sec of post-paw movement (Fig 8a). Across all video recorded sessions we identified between 13,757 and 124,397 left paw movement bouts in individual mice (i.e. times where the left paw moved; see Methods; number of movements in all mice: M1: 54016; M2: 16241; M3: 18186; M4: 20487; M5: 13757; M6: 124397). We then ranked every left paw movement bout by the longest period of non-lever pull activity, i.e. we ranked paw movement bouts by the amount of lever pulls occurring in the previous 15sec or following 5sec (Figure 8a). We next extracted the trials with a complete lever-pull lockout (i.e. no lever pulls 15sec before or 5sec after) and added the locations of left and right paw movements and licking events (Fig 8b). We then realigned the surviving bouts by the longest period of body movement quiescence, i.e. we reranked the remaining paw movement again by quiescence (Fig 8c). Finally, we looked for left paw movements that were not preceded by any movements for at least 5sec. (Fig 8d). This approach revealed between 96 to 557 left paw movements that had at least 5sec of

no preceding body movements and were completely isolated from lever pulls (number of movements per mouse: M1: 416, M2: 96, M3: 133, M4: 167, M5: 177, M6: 557).

Neural activity increases one to two seconds prior to left-limb movement. We next computed the average neural dynamic for the right hemisphere motor, upper-limb and retrosplenial cortex activity and found that both motor and upper-limb cortex exhibited a slow rising time course commencing at approximately -2sec prior to paw movement, with the upper-limb cortex signal being larger than motor cortex (Fig 8e for example from mouse M1). We computed the upper-limb cortex average signal for all animals and found that in 4 mice (M1, M3, M4, M5) this signal showed a significant increase prior to movement (i.e. rising above 3 x the standard deviation of the preceding neural activity) commencing approximately -2sec to -1sec relative to paw movement time (Fig 8f). Mouse M2 had an average [ca] signal which was noisy, likely due to the lower number of trials. Mouse M6 also had a noisy signal that showed an increase above 3 x std prior to movement, but not as pronounced as the other 4 mice. We note that mouse M6 had more than 5 months of recording and the pooled trials likely reflected significantly more variance due to pooling bouts from longitudinal data (see Figure 2, figure supplement 3 and Methods for a detailed discussion on the challenges of pooling widefield [ca] data across long periods of time). We also sought to decode upcoming behavior-locked out paw movements but found that SVM-based methods did no better than chance (not shown). This was likely due to higher dynamics occurring during non-goal oriented paw movements, but we also could not rule out the effect of pooling only a few hundred trials from tens of thousands of trials across many months of recording (see also Discussion).

Computing the average neural signals in motor, upper-limb and retrosplenial cortex from the means in all mice we found that both motor and upper-limb cortex showed a significant increase in the average neural signal beginning at approximately 2sec prior to paw movement (Fig 8g). In contrast, the average

neural signal in these areas prior to water rewarded (locked-out) lever pulls showed a decrease commencing as early as -5sec prior to lever pull (Fig 8h).

In sum, we find that prior to non-lever pull related and isolated left paw movements, the [ca] neural activity in mouse motor cortex begins to increase at approximately -2sec to -1sec prior to paw movement - consistent with human EEG studies on the readiness potential dynamics occurring prior to spontaneous finger or hand movement. In contrast, self-initiated water rewarded lever pulls contain an inhibitory signal that starts earlier, at approximately -5 to -4 seconds prior to lever pull and contains stereotyped neural patterns that can be decoded to predict upcoming level pull timing (see Figures 1,2 and 6).

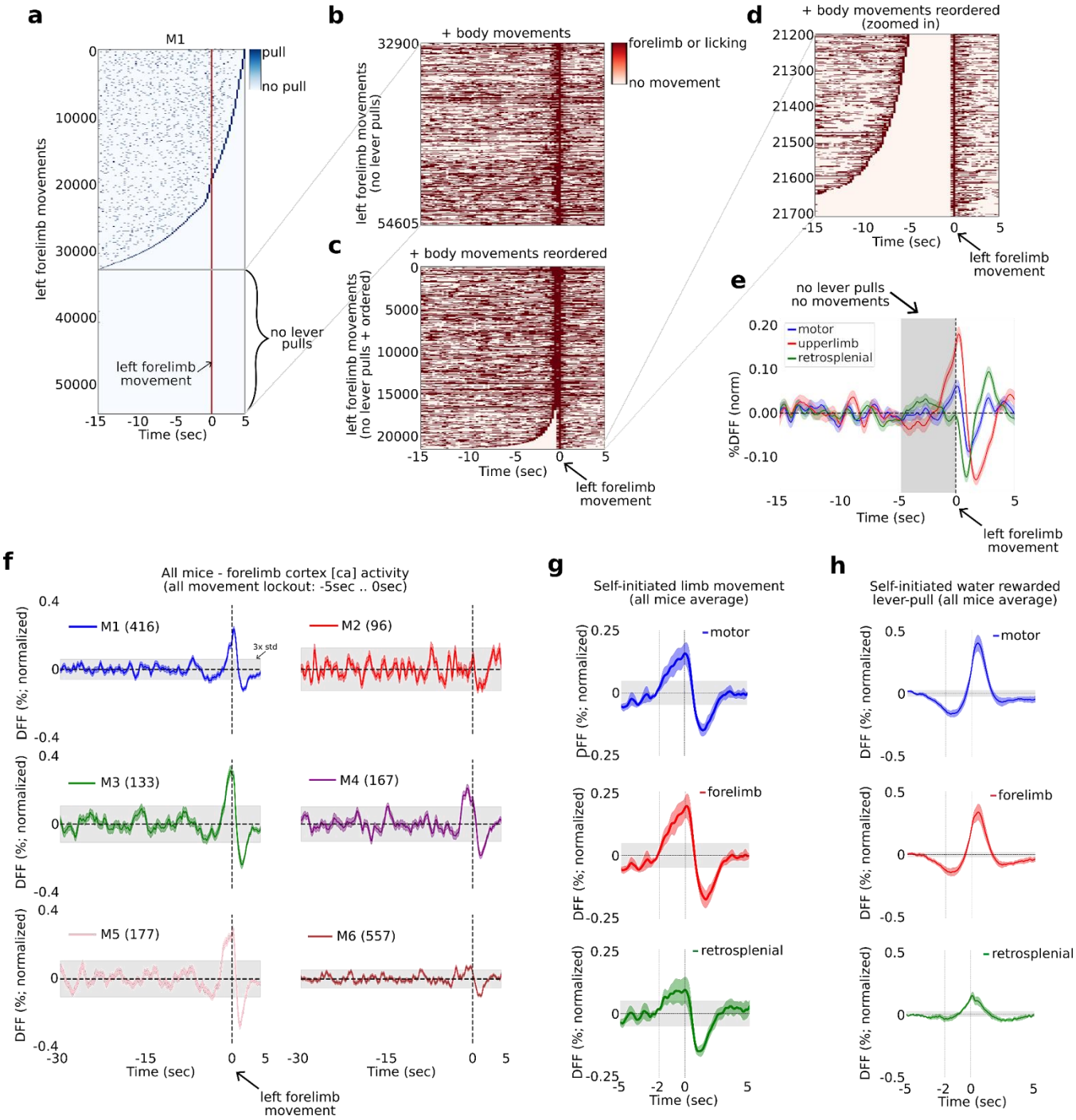

Figure 8. The widefield [ca] activity correlates of random vs. goal-oriented self-initiated actions.

(a) Raster plot showing the location of all lever pulls in mouse M1 across all sessions (blue rasters) relative to spontaneous left paw movements (red line at t=0sec) ordered by the duration of pre-paw-

movement lever-pull quiescence. (b) The completely lever-locked left forelimb movements from (a) with added left and right forelimb movements and licking events (red rasters). (c) Same as (b) but ordered by the duration of quiescence prior to the left forelimb movement. (d) The bottom events from (c) showing the location of left and right forelimb movements and licking events (red rasters). (e) The average neural dynamics in motor cortex (blue), forelimb cortex (red) and retrosplenial cortex (green). (f) The average forelimb cortex activity (color shading represents standard error) for each mouse during periods as in (d) and (e). (g) The average neural activity (color shading represents standard error) from all mice averages as in (f) for motor, forelimb and retrosplenial cortex. (h) Same as (g) but for water rewarded lever pull activity. (Note: gray shading in all plots represents 3 x standard deviation of the average neural signal between -30sec to -5sec prior to movement or lever pull; see also Methods).

DISCUSSION

Since the 1960s, several human neuroscience studies seeking to identify the neural correlates and genesis of self-initiated, voluntary action have found that increases in neural activity in SMA and preSMA precede both voluntary movement and even awareness of the intent to act (Kornhuber and Deecke 1965; Libet et al 1983). Most studies found only small differences (~150 ms) between the intent to act and voluntary action initiation; however, these findings remain controversial and determining the precise arrival of subjective intent and the effect of reporting it is a complex topic (see e.g. Wegner 2002; Dijksterhuis et al 2006; Tusche et al 2010; Sinnott-Armstrong 2010; Dijksterhuis and Aarts 2010). Removing the reporting of intent from voluntary behavior paradigms and focusing solely on the relationship between neural activity and self-initiated action avoids some of the controversies and focuses the debate on the study of objective variables (e.g. timing of behavior initiation, neural activity in specific areas) - and enables the use non-human animal models for self-initiated and voluntary action research.

Self-initiated actions in mice are prepared seconds prior to movement and are biased to occur during specific phases of slow oscillations. Using a self-initiated behavior paradigm in mice to relate pre-movement neural activity to the initiation of behavior enabled us to collect a high number of behavior trials across weeks and months of recording and with higher neuroanatomical resolution recordings than EEG and higher temporal resolution than fMRI. Self-initiated behaviors in mice were preceded by a decrease in widefield [ca] neural activity starting 3-5 seconds prior to behavior time, similar to (but longer) than the EEG RP signals in humans (Fig 1, see also Kornhuber and Deecke 1965; Libet et al 1983). We further found that decoding of upcoming behavior approximately three to seven seconds prior to movement was possible, a finding consistent with findings using fMRI in humans (Soon 2008; 2013; Bode et al 2011; see Figs 1,2). Self-initiated behaviors were even more biased towards specific phases of neural activity than in humans (Fig 3). This suggests that in mice, oscillation phase

could be even more determinative of action initiation timing than in humans. Overall, these results link human voluntary action studies with rodent self-initiated behavior studies and suggest mice as an adequate model for studying the neural correlates of self-initiated action.

Behavior preparation signals are distributed across the cortex. While the vast majority of voluntary action studies in humans focused on SMA (and preSMA), we found that decoding future behaviors using motor (or limb cortex) was inferior to decoding using all cortical activity (Fig 2). This suggests that pre-voluntary movement neural signals are widely distributed across the dorsal cortex but also that more temporally and spatially precise neural recordings may be required for a complete characterization of pre-movement neural activity in humans (and non-humans). Coupled with a neural recording modality that more precisely reports local neural activity (i.e. widefield [Ca++] cortex) our findings suggest that voluntary action studies in humans may benefit from subcranial neural signals from multiple areas.

The role of motor cortex inhibition prior to lever pulls. Our paradigm shows that, on average, motor cortex is inhibited beginning approximately -5sec prior to lever pulls. In some mice and sessions, we found EDTs as low as -7sec which suggest the inhibitory (and other dynamics) commence even earlier. In parallel, we found that mice decreased, but not stopped altogether, random body movements during the period of -5sec to 0sec. While our task did not require mice to cease body movements prior to lever pulls, it is possible that preparation of future pulls requires some mesoscale inhibition of motor cortex which necessarily leads to decreases in body movements. This hypothesis of delays in behavior on the order of seconds has some support from studies which show human subjects are more likely to initiate actions during exhalation periods which are generally 3 seconds in duration (Park et al 2020), although mice breath faster than humans. Another interpretation is that mice consciously inhibit motor cortex in preparation of an action towards a water reward. (We use the term consciously, as we view intentional inhibition as achievable via unconscious systems). For example, for every lever pull mice

consciously withhold pulling the lever prior to movement as they learn to “count” several seconds prior to carrying out an attempt at the lever pull. In our opinion, this “counting” might occur consciously or subconsciously and it would be challenging to establish in humans let alone in mice where we lack subjective report. In addition, such a strategy might lead to higher variances in the duration of inhibitory bouts - yet the neural dynamics of 15sec lever-pull lockout trials were sufficiently stereotyped to yield EDTs on the order of multiple seconds. Additionally, one mouse (M1) in our study did not internalize appear to learn the 3sec lockout rule and did not persevere at lever pulls at approximately 3sec intervals, yet had decodable EDTs. However, we cannot rule this possibility out with our dataset and paradigm. Such an interpretation could also call into question whether volitional actions towards a highly-salient goal can be studied at all in the lab under self-initiated or self-paced paradigms. That is, it would raise the question of whether the study of volitional action towards high-value (rather than low-value) goals can only be carried out in natural settings where the opportunity for high-value decisions arises naturally from internal states rather than as part of an instructed paradigm.

A simpler explanation for our results is that the inhibitory dynamics are an integral part of preparation of a future action towards a salient goal and that they are present prior to action towards a salient goal in other paradigms. The duration and extent of such dynamics may be different than our paradigm where we required a 3sec lockout, but could be detected in both rodents and humans acting volitionally towards a highly salient goal.

Comparison of our study with cued action studies. In our experience, mice following external cues such as a light or sound triggers initiate their behaviors immediately and decoding the timing of future behavior on the scale of seconds is not possible. However, it is possible that in cue-triggered experiments - expert mice exhibit motor cortex inhibitory signals while they are waiting for a cue (e.g. see Schurger et al 2012). However, such neural states would be conditioned on the eventual arrival of an external cue towards a future action and would not constitute self-initiated volitional action. Another

possible paradigm would be to train mice to withhold action following a cue for several seconds prior to movement. In such a paradigm the neural correlates of action inhibition would be the focus rather than preparation of future action. Lastly, optogenetic approaches to activate or inhibit motor and forelimb cortex of mice after they have acquired the task could also be implemented, especially if mice learn a self-initiated - rather than cued task (the latter being more often the case). Overall, we view these and other similar paradigms as useful complementary studies to our work and suggest them for future studies.

Longitudinal performance of a self-initiated task restructures the neural dynamics underlying action and spontaneous neural activity. It has been suggested that noise-driven stochastic models (i.e. leaky stochastic accumulators) can explain the RP as a result of averaging backwards in time over multiple stochastically determined behavior initiations (Schurger et al 2012). In contrast, a recent human study aimed at testing part of this hypothesis found that the RP amplitude increased with learning suggesting that the RP represents planning and learning rather than stochastic structures alone (Travers et al 2021). Consistent with the later study, we also found that decoding times for upcoming water rewarded lever pulls in some mice changed, in particular they became shorter (Fig 4). We also found structural changes in the neural dynamics in some mice as both the lever pull neural space and its overlap with the left-paw changed systematically with time. These results suggest that learning, or merely longitudinal performance, of a high-value behavior (e.g. water seeking in water deprived mice) increases stereotypy even in self-initiated actions. We suggest that automaticity-like processes could be involved with movement preparation becoming less dependent on cortex and more dependent on subcortical structures. These large-scale cortical changes in brain activity have been observed in humans, for example, while learning a brain-machine-interface task (e.g. Wander et al 2013) but aside from a very recent EEG study (Travers et al 2021) are not well described. The mesoscale mechanisms for such changes may involve increased representation of lever-pull preparation dynamics in the overall

spontaneous dynamics (e.g. occurring more frequently) or increase differentiation between lever-pull preparatory neural activity and other behaviors. These results add to the evidence that self-initiated actions are supported by learned neural-dynamical structures and that those can change on longer time scales.

Inter-animal variability. We found inter-animal differences in several results: different decoding times, anatomical areas involved as well as longitudinal dynamics (e.g. differences in longitudinal decoding trends Fig 4; or preferred phase angles at behavior time different Fig 3; different trends in frequency peak and power Fig 7). These results suggest that neural dynamics and strategies for initiating a self-initiated action could be specific to individual subjects and that pooling over multiple subjects may remove novel or important differences. In other words, single subject analysis may be critical to further advancing the debate on the dynamics of neural activity underlying self-initiated behaviors in both humans and nonhumans.

Internal state evidence accumulation commences seconds prior to movement. We found that both lever-pull decoding accuracy increases nearly monotonically with approaching action (e.g. Fig 4b) and that intra-session variance decreases several seconds prior to movement within limb, motor and retrosplenial cortex. We suggest these findings constitute further "indirect evidence that evidence-accumulation" (Boid et al 2014) is occurring even in the absence of explicit stimuli - likely based on evaluations of internal states and models. This supports the hypothesis that internal-state driven self-initiated actions could be potentially modeled by commonly used perceptual and cognitive decision making models (Gold and Shadlen, 2007; Heekeren et al. 2008; Murakami et al 2014, 2017).

The effect of confounding movements on the decoding of future rewarded action. Our study does not directly address the effects of stimuli or other perturbations on the neural dynamics preceding self-initiated decisions, for example, as in some human choice paradigms that consider decision choice in the presence of novel information (e.g. Maoz et al 2019). Additionally, there is evidence that micro-

movements can contribute to ongoing neural activity between behavior bouts (Stringer et al. 2019 and Musall et al. 2019). While it is possible that in preparing for a self-initiated rewarded behavior mice undergo a series of physical movements, we did not see any evidence for this in our recordings. In particular, we found a tendency for mice to decrease their body movements in the 3-5 seconds prior to self-initiated action and we did not find evidence for sequences of paw or licking movements. We suggest future studies focusing on the micro-movements underlying self-initiated action could address this issue using high-frame rate and high-resolution video recordings.

Limitations. Our study focused on characterizing *neural dynamics* and *timing* of an ethologically valuable movement rather than identifying *intent* or *awareness* of upcoming movements. As such, we do not directly address the role of subjective "intent" as in some human EEG studies (e.g. Libet et al 1983) or the role of reasons or deliberation on decision making (Note: as mentioned above, the effect of reporting intent and the use of reasons or deliberation in voluntary actions are the subject of ongoing debates; see, for example, Dijksterhuis et al 2006; Dijksterhuis and Aarts, 2010; Vierkant et al 2019; Wegner et al 2002). Our study was also not aimed at disambiguating between the timing of intent awareness and movement. Uncued voluntary action studies in humans generally find the difference between the timing of subjective intent and movement to be small (e.g. 150ms; Libet et al 1983) or even negligible, orders of magnitude smaller than the EDTs in our results. Second, our decoding times showed a strong dependence on the *number of trials* suggesting that additional trials would change (most likely improve) our decoding results (though we note that this effect may merely reflect sequences of lever pulls). Although it is challenging to keep animals motivated across many trials within a single ~20min session, decreasing reward size might have increased the number of self-initiated lever pull behaviors and reduced the dependence we observed. Third, we sought to remove pre-movement confounds from our results by "locking out" previous lever-pulls or body movements (Fig 6). A more direct approach where animals are specifically trained to remain quiescent prior to an action may yield

more trials and easier to interpret results. However, it is practically challenging to train mice to withhold behaviors for significant periods of time (e.g. >> 3sec) while also performing a task for a valuable reward. Fourth, we found strong correlations between lever pulls and body movements in all mice (not shown). However, we did not take into account the temporal location of lever pull activity when decoding the body movement (Fig 2); for example, we decoded upcoming left paw movement initiations without accounting for - or removing - lever-pull initiations co-occurring with such paw movements. It is obvious that many of the spontaneous paw movements also coincided with lever-pulls and thus the EDTs for paw movements were not an independent measure from the EDTs of rewarded lever-pulls. However, we chose to remain agnostic and not separate body movement initiations into those coinciding with lever pulls and those that occurred many seconds away from rewarded lever pulls (this also had the effect of preserving a higher number of body-movement trials for decoding). Despite not separating the data, we did find a significant difference in lever pull and right paw dynamics longitudinally (Fig 4j) suggesting that further separation may have only increased this difference. We acknowledge that it would have been interesting to divide the behaviors and carry out separate analysis, and leave this direction for future projects.

Conclusion. Over the past few decades rodent models of sensory systems and decision making have become increasingly common (e.g. visual evidence accumulation; Najafi and Churclhand 2018; Odoemene et al 2018; IBL et al 2021). The findings presented here suggest that mice could also be an appropriate model for neuroscience investigations into self-initiated action. While characterizing the dynamics underlying self-initiated behavior in rodents may advance our understanding of self-initiated action in nonhumans as well, it could also advance our understanding of developmental and psychiatric disorders that have behavioral symptoms such as avolition in depression (e.g. lack of will to move; Brakowski et al 2017) and behavior repetition observed in obsessive-compulsive-disorders (Lysaker et al 2018). Our findings suggest that the neural mechanisms underlying self-initiated action preparation

and performance could be preserved in part, or in whole, between humans and mice and that studies of self-initiated action in humans would benefit from mouse models and the vast libraries of behavior, genetic and neural recording methodologies available.

MATERIALS & METHODS

Mice. Mouse protocols were approved by the University of British Columbia Animal Care Committee and followed the Canadian Council on Animal Care and Use guidelines (protocols A13-0336 and A14-0266). Six GCaMP6 transgenic male mice (Ai93 and Ai94; Madisen et al 2015) were used. For the study the mice names were defined as M1-M6 and had the following genotypes: M1 - M5: Ai94; M6 - Ai93.

Lever pull task. Mice were kept on a restricted water schedule as previously described (see Silasi et al 2016). Briefly, mice were implanted with a head post and head fixed with their bodies partially resting in a 28mm diameter Plexiglass tube. A 1cm cutout from the right side of the tube floor accommodated a monitored lever that was positioned at the same height as the tube. At the start of each session a water spout was set near the mouth of the mice, ensuring the mice could obtain dispensed water drops by licking. In order to receive a water reward mice were required to pull the lever past a threshold and then hold the lever without pulling it to the maximum value. Correct lever pulls - "rewarded lever pulls" - were tracked in real time to provide water reward. Following a reward a lockout period of 3 sec was implemented during which mice could pull the lever but would not be rewarded irrespective of performance. This task required learning the minimum threshold, the duration of the hold and the refractory period of the lockout. We note that the duration of the hold was gradually increased by 0.1sec increments in mice that learned to perform the task well. We selected 3 seconds as longer lockout values limited the consistent acquisition of the lever pull task. We recorded widefield calcium activity across each recording session (1330 sec, i.e. ~22mins long) over many days (42-109 days, average = 58.3 +/- 24.6 standard deviation). Mice had longitudinal trends with some increasing the # of lever pulls over time and others decreasing (See Fig 4a; M1-M6: pearson correlations: -0.25, 0.39, 0.65, -0.37, 0.18, 0.68; p values: 0.048, 0.020, 1.095e-5, 0.288, 6.320e-15; Note: because mice were not habituated we

discarded the first week of training in this computation to better capture longitudinal trends rather than habituation idiosyncrasies).

Widefield Calcium Imaging. Widefield calcium imaging was carried out as described previously (Xiao et al 2017; Silasi et al 2016). Briefly, mice with a chronically implanted transcranial window were head fixed under a macroscope. Images were captured at 30 Hz with 8x8 pixel binning, producing a resolution of 68µm/pixel (Vanni and Murphy, 2014). To visualize the cortex, the surface of the brain was illuminated with green light (but not during image acquisition). Calcium indicators were excited with blue-light-emitting diodes (Luxeon, 470 nm) with bandpass filters (467–499 nm). Emission fluorescence was filtered using a 510–550 nm bandpass filter or collected in a multi-band mode as described below. For single wavelength green epifluorescence, we collected 12-bit images at varying time resolution (33 ms; i.e., 30 Hz) using XCAP imaging software. In order to reduce file size and minimize the power of excitation light used, we typically bin camera pixels (8 × 8) thus producing a resolution of 68 µm/pixel. Hemodynamic correction was not available as we only used single wavelength excitation. Based on previous experiments using similar imaging conditions (Vanni and Murphy 2014, Silasi et al. 2016, Vanni et al. 2017) in control GFP expressing mice we would not expect significant contributions from hemodynamic signals under the conditions we employed. These imaging parameters have been used previously for voltage-sensitive dye imaging (Mohajerani et al., 2013) as well as anesthetized GCaMP3 imaging of spontaneous activity in mouse cortex (Vanni and Murphy, 2014) and awake GCaMP6 imaging in mouse cortex with chronic window (Silasi et al 2016).

Behavioral recordings. Behavior was recorded using a Windows OS camera at 15 frames per second. Video recordings were saved in the native .wmv format and converted at the same resolution to .mp4

format for post-processing steps. Each video recording session lasted approximately 22 minutes and contained ~20,000 frames.

$\Delta F/F_0$ computation. $\Delta F/F_0$ computation was carried either via bandpass filtering (0.1Hz to 6.0Hz) or as previously described (Xiao et al 2017). Briefly, F_0 was computed as the average pixel activity in the window preceding the analysis window. For example, for analyses of neural activity within a +/-3sec window following a behavior, F_0 was computed based on the previous 3 sec of neural activity, i.e. the -6 sec to -3 sec window. We found no statistical differences in our results between using sliding window $\Delta F/F_0$ or bandpass filtering and for our analysis we relied only on bandpass filtered data.

Registration to Allen Institute dorsal cortex map. We used a 2D projection of the Allen Institute dorsal cortex atlas, similar to Musall et al., 2019, Saxena et al., 2020 and Couto et al., 2021 to agnostically identify ROIs without the need for stimulus driven or other neuroanatomical markers. We rigidly aligned the widefield data to a 2D projection of the Allen Common Coordinate Framework v3 (CCF) (Oh et al., 2014) as in Musall et al., 2019, Saxena et al., 2020 and Couto et al., 2021, using four anatomical landmarks: the left, center, and right points where anterior cortex meets the olfactory bulbs and the medial point at the base of retrosplenial cortex. The ROI's identified for each animal and session were individually inspected to qualitatively match expected activation of somatosensory cortex during lever pull trials in each session.

Analysis. All analysis was carried out using custom python code developed as part of an electrophysiology and optical physiology toolkit available online (https://github.com/catubc/widefield). Methods for computing event triggered analysis for widefield imaging have been previously published (Xiao et al 2017) and are also available online (https://github.com/catubc/sta_maps).

Unsupervised behavior annotation and body movement computation. Seven features were identified for tracking: center of left paw, center of right paw, the underside of the jaw, the tip of the nose, the underside of the right ear, the tongue and the midpoint of the lever. DeepLabCcut (DLC v. 2.1.8; Mathis et al 2018) was used to label these features in 60 frames per video for 3 videos in each animal. The DLC predictions were inspected and smoothing was applied to correct missing or error frames (using a 30 frame window sliding mean or Savitsky-Golay 31 frame filter using 3rd degree polynomial; note mouse M2 did not have good tongue tracking and this feature was excluded from analysis). Body movement initiations were computed as the first time point at which the velocity was larger than 3 times the standard deviation of velocity over all periods. We then excluded movement initiations which were preceded by another initiation (of the same body part) in the previous 3 sec of time.

Principal Component Analysis. PCA was applied to neural activity time series to decrease the dimensionality and denoise the data. For each session we first converted the filtered [Ca++] neural activity from pre lever neural recordings from time -15 sec to + 15 sec into a series of [n_frames, width_pixels * height_pixels]. This data was then run through principle complement analysis linear dimensionality reduction using the python sklearn package to obtain a pca model (https://scikit-learn.org/stable/modules/generated/sklearn.decomposition.PCA.html). We next selected the number of principal components required to reconstruct the data to >= 95% variance explained precision. Lastly, we applied the PCA model (i.e. denoised) to both the lever-pull neural data and control data.

Support vector machine classification - decoding single sessions. We used SVM classification to decode neural activity preceding an action vs random periods of time using methods similar to those used in humans with functional Magnetic Resonance Imaging data (fMRI; Soon et al 2008). Briefly, for

each session and each rewarded lever pull or body movement initiation we extracted segments of neural activity 30sec long centered on the time of the action (i.e. -15sec to +15sec following the action). Controls were selected similarly but the time of the action (i.e. t=0sec) was randomized to fall anywhere in the session except a +/-3sec window around an action. For clarity, controls could contain neural activity from rewarded lever pulls or body initiations; we found this to be a more conservative method than to manually select only non-movement periods as controls. We next denoised both the behavior data and the control data using PCA (see description above). We then built SVM classifiers using as input 1 sec-wide windows (30 frames @ 30 FPS) of data from both the behavior (i.e. class #1) and the random controls (i.e. class #2). The input to each SVM classifier was a 2D array [n_trials, n_frames * n_PCs]. For example, in a session where >95% of the data dimensionality was captured by 10 PCs, the input the the SVM classifier was: [n_trials, 30*10] = [n_trials, 300]. We similarly computed the control array and the SVM classifier was trained on two classes (i.e. lever pull vs. control). We tested additional sized windows (i.e. single frame=30ms, or 150 frames = 5 sec) but did not see significant improvements. We used sigmoidal SVM kernels as they showed a slight improvement in SVM accuracy over linear kernels (see https://scikit-learn.org/). We carried out 10 fold cross validation using a split of 0.9:0.1 train:validate. The output of the SVM classification for a 1sec window was assigned to the value of the last time point in the stack (e.g. the accuracy computed from decoding the -15sec to -14sec time window was assigned to the -14sec time bin). We carried out this SVM classification for each time point in the -15sec to +15sec window. For clarity, 870 SVM classifiers (-15 sec to +14 sec = 29sec *30 fps = 870 frames) were trained for each validation point (i.e. 10- fold cross validation).

Support vector machine classification - decoding concatenated sessions. We additionally trained SVM classifiers on concatenated sessions to increase the number of trials available. Sessions were concatenated across sequential behavior days to reach a minimum of 200 trials. Intra-session PCA was

first applied to each session to denoise the data locally (using a minimum of 95% reconstruction accuracy as above. The denoised time series were then concatenated and fit to a PCA model (https://scikit-learn.org/stable/modules/generated/sklearn.decomposition.PCA.html) using randomly sampled (3%) of the data from the concatenated stack. The multi-session PCA matrix was then used to denoise the individual sessions and we kept a fixed 20 principal components to reconstruct the concatenated datasets. The remaining steps (SVM training and decoding) were carried out as for the single session approach described above.

Support vector machine classification - decoding locked out concatenated sessions. We trained SVM classifiers on trials that were locked out (i.e. not preceded by a previous rewarded or unrewarded lever pull) by several seconds (see Figure 6). Sessions were generated by pooling a minimum of 50 to a maximum of 200 locked-out trials. We chose these values to be qualitatively similar to the analysis done for non lockout trials in which we used single session trials (ranging from 30 to > 100 trials per session) and concatenated trials (which contained trials from several sequential sessions reaching a minimum of 200 trials). We used a 50 trial-sliding window to select trials for each concatenated session. For example, for mouse M1, for a lockout of 15 sec, a total of 503 trials survived out of all rewarded lever pull trials. We pooled these 503 trials in groups of 200 using 50 trial windows resulting in 10 groups of (overlapping) data to be processed (i.e. 0-200, 50-250 … 450-503). This method is essentially similar to the concatenated datasets where for each session we added trials from subsequent sessions until we reached at least 200 trials (i.e. that method also yielded overlapping trials across time). While this method does yield overlapping trial sessions, our goal was to show EDTs for such synthetic sessions. Using non-overlapping data (i.e. the sliding window was set to 200 trials) yields similar results.

Computation of Earliest Decoding Time (EDT). We sought to use a method that detected the first time point in the cross-validated SVM accuracy curves that was above chance at a statistically significant level (i.e. student t-test p value < 0.05). We denoted this time as the Earliest-Decoding-Time (EDT) for each session. We obtained the EDT for each session using several steps. First, for each session, we computed the 10- fold cross validated accuracy curves using 30-time step (i.e. 1sec) windows (as described above but we additionally filtered the accuracy curves using a 30-time step moving average to further decrease the effects of noise on the prediction curves. Next, we obtained the significance at each time point by computing a 1-sample t- test between the SVM cross validation accuracy values (i.e. 10 values) and a population mean of 0.5 (i.e. chance) using the python scipy stats package. We next applied a Benjamini-Hochberg correction for multiple tests using the python statsmodel package. Finally, starting at t=0 sec, we moved backwards in time until we found the last time point that was statistically significant (i.e. p value < 0.05 as computed above). This last step had the effect of imposing a constraint which required all decoding accuracy distribution times following the EDT to be statistically significant - thus excluding random stochastic fluctuations in the accuracy curves which could result in very low EDTs that are not reasonable or meaningful. The effects of this last constraint could be observed in Figs 2g,h where the EDT is higher (i.e. closer to t=0sec) than other time points that are statistically significant (see top colored bars for statistical significance and note that there are some isolated times that show statistical significance). We denote “shortened” EDT time to indicate that the EDT time to the lever pull time (i.e. t=0sec) decreased (i.e. decoding become poorer) and “lengthened” EDT time to indicate that the EDT time to lever pull time increased (i.e. decoding was better).

Statistical tests for single ROI vs. all neural areas. 2-Sample KS tests were carried out between EDTs obtained by using limb cortex neural activity vs. EDTs obtained using all areas. This analysis was done on non-lever lockout data (i.e. all rewarded lever trials) as it is a cross-feature analysis not a cross-

session analysis and we were interested in the relative effects between areas not absolute EDT times. This approach enabled us to obtain a significantly higher number of sessions (as opposed to using locked out data only).

LocaNMF: LocaNMF was applied to the data from each widefield session as in Saxena et al., 2020. Briefly, we applied semi non-negative matrix factorization (sNMF) to the denoised data, while encouraging localization in the spatial components to the Atlas regions. This results in spatial components that are aligned to the different Atlas regions, thus allowing us to further analyze the corresponding temporal activity in each region. The locaNMF parameters used were as follows: maxrank = 1; min_pixels = 200; loc_thresh = 75; r2_thresh = 0.96; nonnegative_temporal = False; maxiter_hals = 20; maxiter_lambda = 150; lambda_step = 2.25; lambda_init = 1e-1.

Power spectra. LlocaNMF temporal component spectra was computed using the python scipy signal package.

Low band-pass filtering of time series. We used both causal and non-causal filters to evaluate the effects of filtering on EDTs. For non-causal filtering we used the scipy.signal.filtfilt(), and for causal filtering we used scipy.signal.lfilter() and corrected by shifting the filtered time series by an amount of fps x 1/filter_frequency = 30fps x 1/0.3hz = 100 time steps. Both filtered time series were qualitatively similar in shape, amplitude and phase.

Convex-hull analysis. For each session, the neural activity "convex hull" at lever pull time (i.e. t=0 sec) was defined as the hyper-volume that enclosed the t=0 sec neural activity vectors. As convex hull analysis is sensitive to outliers a 10% K-nearest-neighbor triage was implemented prior to evaluation.

The convex hull of lever-pull (i.e. t=0 sec) neural activity can be visualized in two dimensions by carrying out PCA on all the neural activity from the session and then computing the convex contour enclosing the t=0sec neural activity vectors (See Fig 4d-blue dots). For computing the ratios of the pre-pull convex hull to the random neural data we chose random periods of time uniformly from the session. The normalized area under the ratio was computed by first computing the convex hull of neural dynamics from -10sec to 0sec prior to a pull, normalizing at every computation by the total area of the convex hull for all neural activity occurring in the session. We then computed the area under this curve and divided it by a similar computed curve by this time starting at randomized times (i.e random times at least 3 seconds away from a rewarded lever pull).

Pre-movement region-basedROI phase computation. We computed the phase of a neural activity of single trial for each region's temporal componentsROI by fitting a sine function to the period of -5 sec to 0sec prior to lever pull. We next computed the phase of each trial as the intersection of the sine fit with the t = 0 sec line.

Sinusoidal fits to single trial data. Sinusoids were fit using scipy curve fit function to single trial neural data from each area based on the last 5 seconds preceding the lever pull (i.e. -5sec..0sec)

Earliest variance decrease time (EVDT). We defined the earliest variance decrease time EVDT for each session as the time at which the variance in a 1sec sliding window decreased by 2 x the standard deviation of the variance computed in the window -30sec to -15 sec prior to the lever pull. We found the requirement for all variance values in a 1sec sliding window to fall below the threshold as necessary to deal with noise or fluctuations in variance. We also required the EVDT to fall between -6 sec and 0.5 sec prior to the pull or it was discarded from analysis resulting in many sessions being discarded from

analysis, especially for mice M1 and M2. More robust methods for detecting the variance decrease are likely possible, but were not explored. We also note that in Mouse M2, the variance change prior to movement was positive (i.e. variance increased) and thus we used the absolute of the difference to compute the EVDT (instead of only considering decreases). We note that as the time courses could be quite noisy, this method is sensitive to thresholds being set, e.g. 2 vs. 4 x std can yield somewhat different distributions. We also note that we used a Savitsky-Golay filter (31 samples) to furter smooth the data in order to get consistent results from visual cortex data.

Detecting stereotyped movements. We sought to detect the presence of stereotyped movement patterns (e.g. left paw followed by right paw followed by licking) using PCA applied to binarized behavior time series (not shown in results). We first obtained DeepLabCut time series locations for the left paw, right paw and tongue as a 2D vector [n_time_points, n_dimensions], where n_time_points: number of imaging frames in a session (usually 1300 sec x 15 fps) and n_dimesions: x and y video coordinates (in pixels). We next generated a boolean array with zeros representing no movement and ones representing body movements. We then extracted segments of 20 sec long around each lever pull (i.e. from -10 sec to +0 sec relative to lever pull) resulting in arrays of dimension [10 x 15fps, 2] = [150, 2]. We then flattened and stacked the arrays (trial wise) and computed PCA on the resulting data (i.e. input into pca [n_trials, n_time_points x dimension]). In an additional step, we also concatenated across body parts resulting in single trial dimensions of [n_time_steps, n_dimensions x n_body_parts]. Neither approach (single body part of concatenated body parts) yielded multiple discernable clusters in the first two PCs.

Quiescence period analysis. Analysis in Figure 1, figure supplement 6, and figure supplement 7 and in Figure 8 required the computation of bouts of activity around a lever pull or limb movement. Movements (of limb or lever) were detected as explained above and binned in segments of 0.250

seconds. Given the lower temporal resolution of our videos, when computing lockouts we allowed for the first or last bin of a lockout period to contain movements (e.g. the first bin in a 15sec lockout period or the very last bin prior to movement, i.e. the -0.250 sec bin).

Processing and analysis of data for Figure 1, figure supplement 7. Pooling data across weeks or months of longitudinal recordings adds substantial noise and other confounds to our datasets (see Figure 2, figure supplement 3, and Main manuscript for Figure 6 for a detailed explanation). For the analysis here we pooled lever lockout trials (as in Figure 6) but were further limited to only those sessions where video was available. This reduced our overall trials by approximately 50% (or more) in all mice compared to Figure 6 analysis. The trials were further split into 3 groups representing least to most body movements. Additionally, trials pooled into these subgroups were ordered by movement amount - as opposed to ordered by day of acquisition time. This also has the effect of increasing the variance of data means due to time between individual trials in the subgroup. Given these issues, our analysis in this panel was limited to characterizing [ca] time courses only (i.e. it was not possible to also carry out EDT decoding on trials contained in these reduced datasets - as the time series were too noisy).

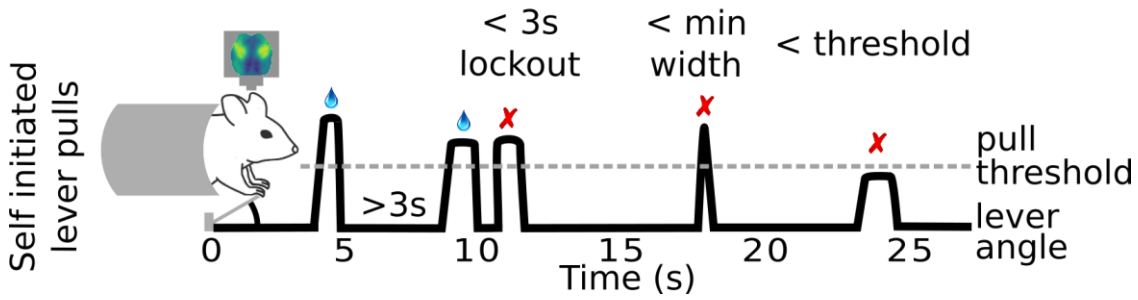

Figure 1 - figure supplement 1: Mouse self-initiated lever pull paradigm. Mice are trained to pull a lever to receive a water reward. In order to receive a water reward the lever pulls must occur at least 3 seconds after a previous lever pull, pass a minimum lever angle threshold, and the lever must be held past the threshold for a minimum amount of time (e.g. 0.1sec).

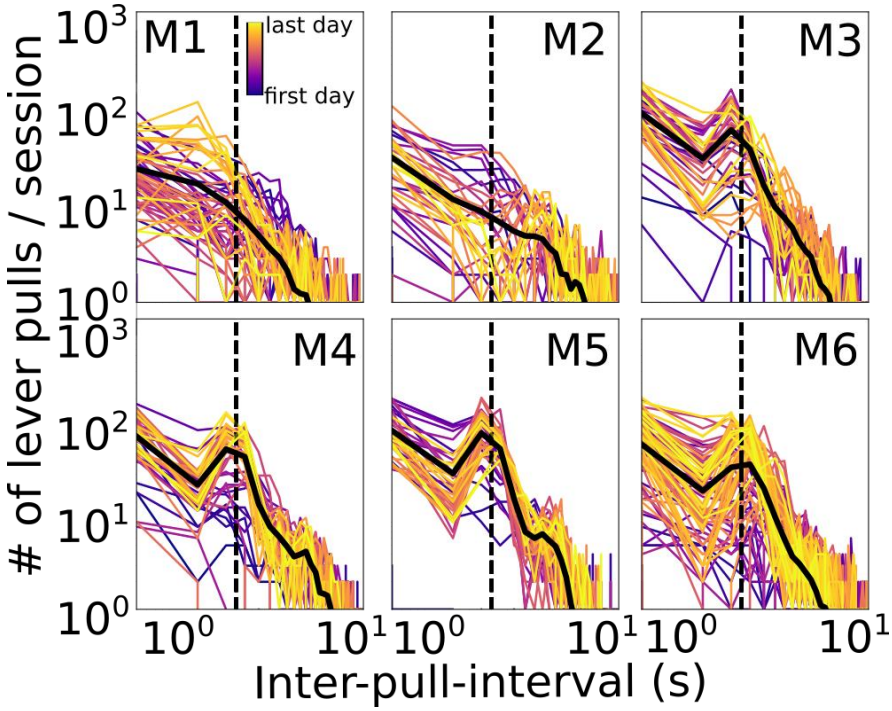

Figure 1 - figure supplement 2: Mouse longitudinal inter-lever-pull interval distributions. Inter-lever-pull distributions for each session (colored lines) and all session averages (black lines) for all mice. Dashed line indicates t=3sec which was the minimum "lockout" time (i.e. no previous lever pull) in order to receive a water reward. (Lever pull times were defined as the initial movement of the lever from rest; see Methods).

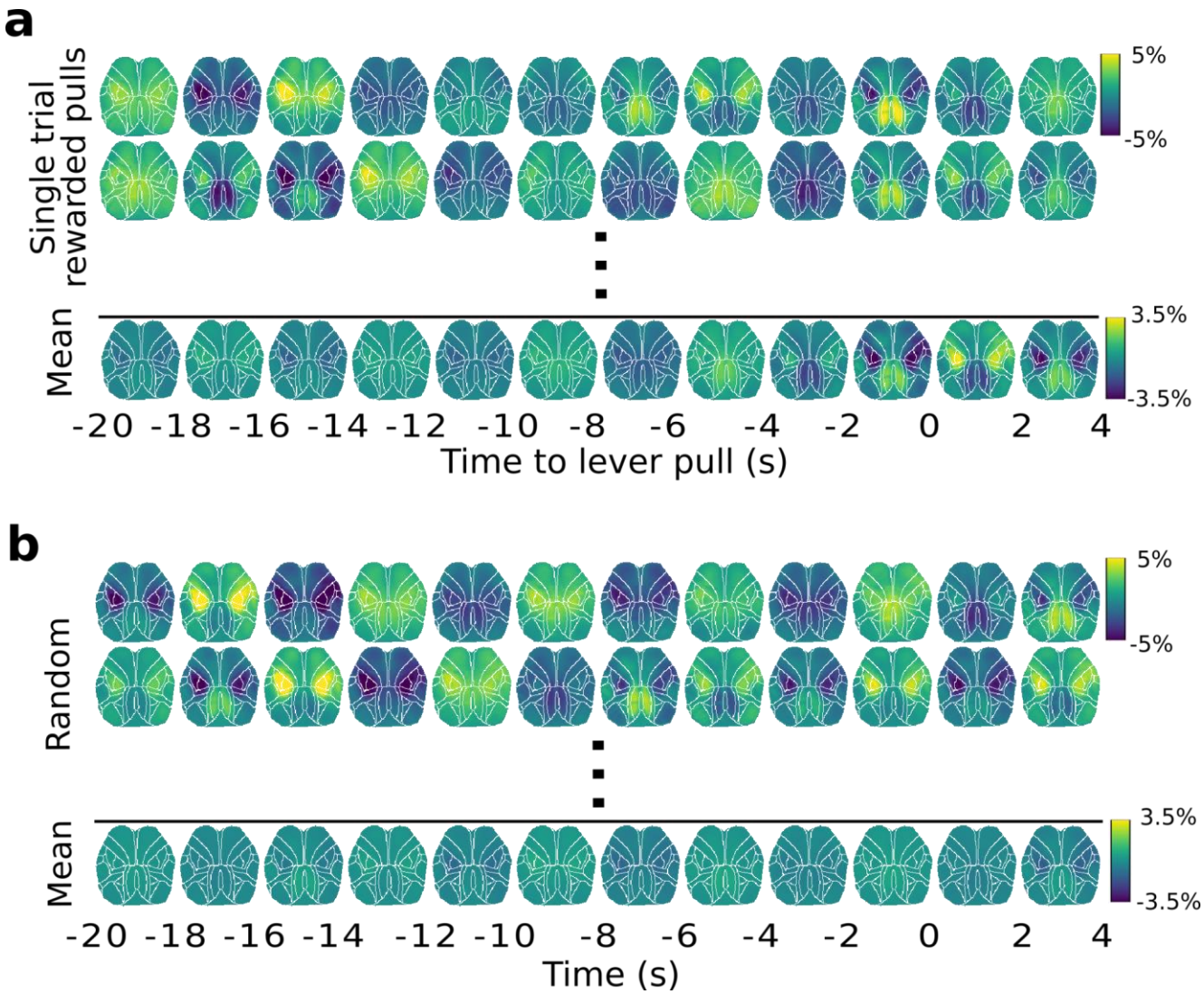

Figure 1 - figure supplement 3: Widefield [Ca++] dynamics during random vs. rewarded lever pulls. (a) Top: widefield [Ca++] activity from single lever pull trials; Bottom: widefield [Ca++] activity obtained for a session average (30 trials). **(b)** Top: same as (a)-Top but for a random segment of neural activity (i.e. not locked to lever pull at t=0sec); Bottom: same as (a)-Bottom but for random neural segments.

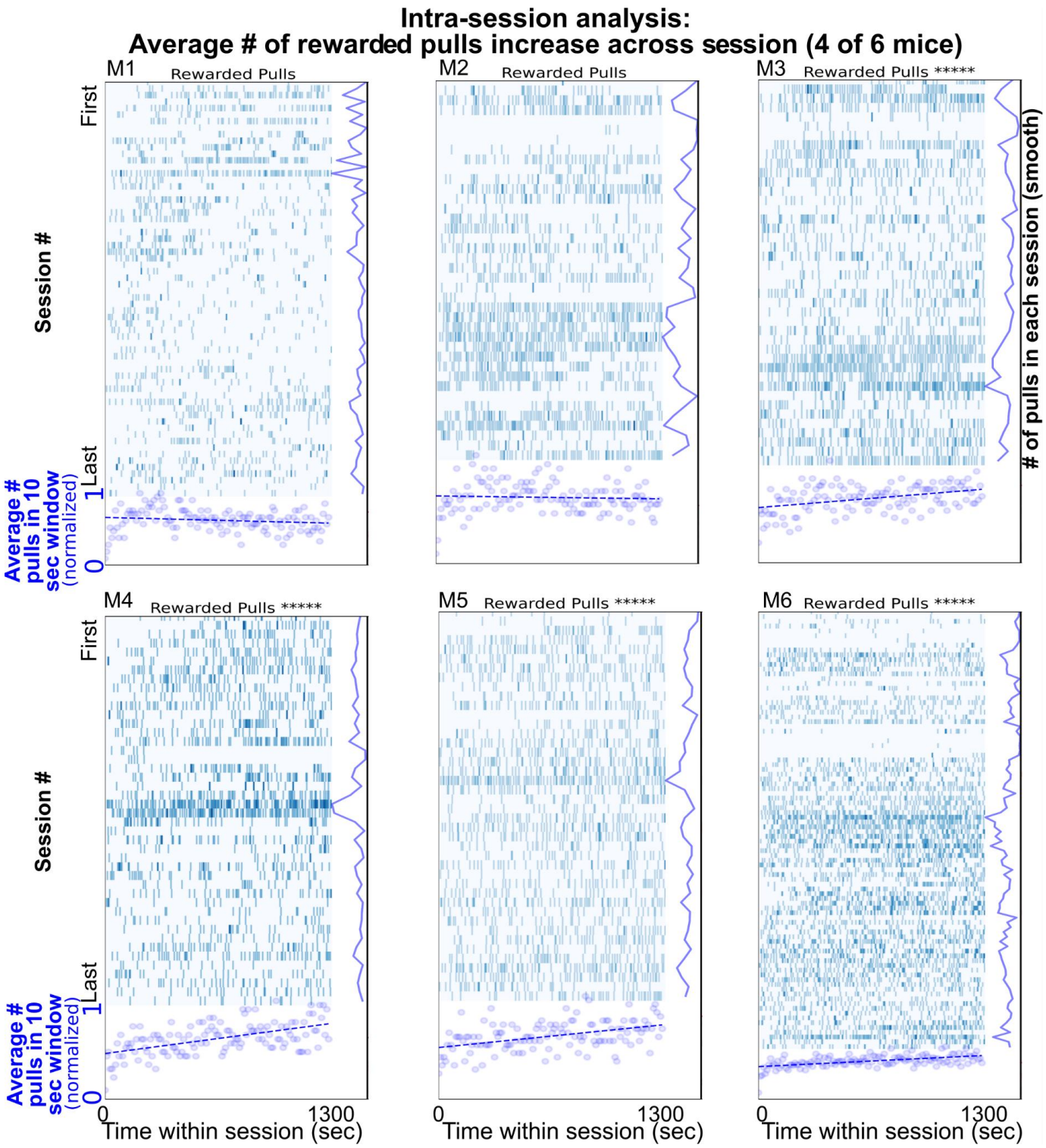

Figure 1 - figure supplement 4: Number of lever pulls changes across sessions. Single lever pulls (blue vertical rasters) and sliding window (10 sec) averages (blue round scatter plot) show that on average four of six mice (M3,M4,M5,M6) increase their lever pulls across the duration of the session

(i.e. have a positive slope in correlation; pearson correlation were: M1: -0.14347 , pval: 0.10479; M2: -0.05616 , pval: 0.52723; M3: 0.38835 , pval: 5.4e-06; M4: 0.55091 , pval: 1.3e-11; M5: 0.44370, pval: 1.4e-07; M6: 0.53118 , pval: 9.4e-11).

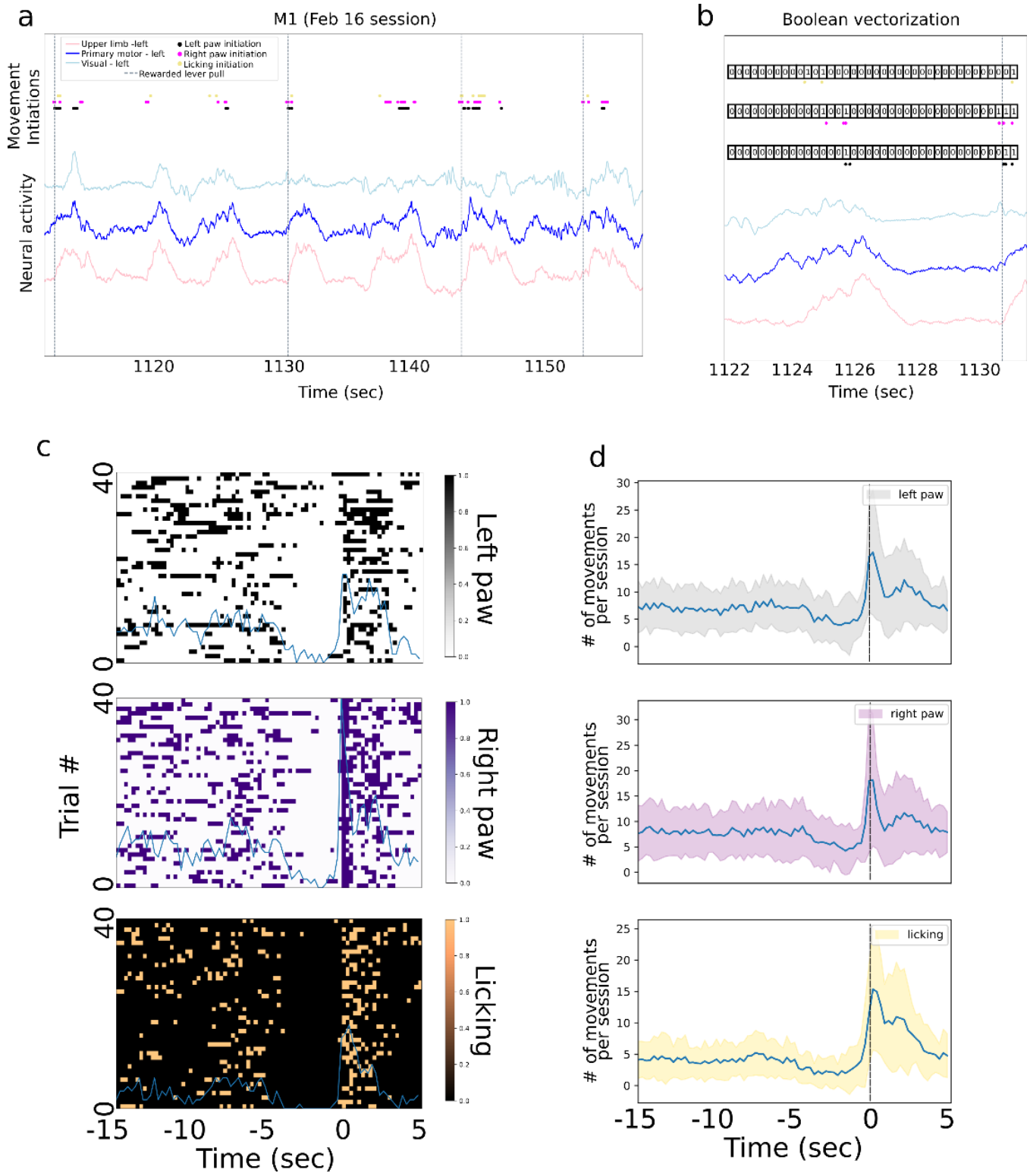
a
M1 (Feb 16 session)
Upper limb -left
Primary motor - left
Visual - left
Left paw initiation
Right paw initiation
Licking initiation
Rewarded lever pull
Movement Intiations
Neural activity
1120
1130
1140
1150
Time (sec)
b
Boolean vectorization
1122
1124
1126
1128
1130
Time (sec)
c
Trial #
40
0
Left paw
Right paw
Licking
-15
-10
-5
0
5
Time (sec)
d
# of movements per session
left paw
right paw
licking
Time (sec)

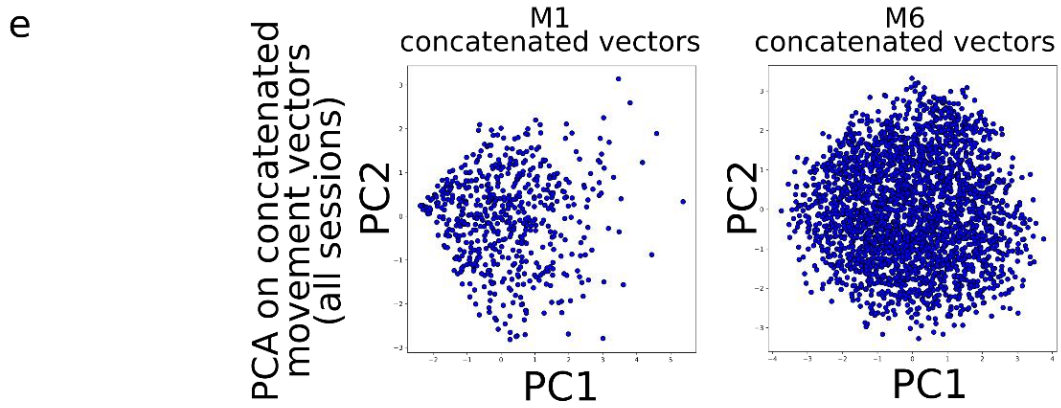

Figure 1 - figure supplement 5: Body movement sequence analysis. (a) An approximately 40 sec period of neural activity from motor, limb and visual cortex overlaid with body movement initiations and rewarded lever pulls. **(b)** A method for detecting sequences of behavior by creating and clustering boolean vectors of activity in 0.25sec bins over the 10 seconds prior to a lever pull. For each body movement initiation (e.g. left paw movement) we created an array containing 0s when the behavior was not present and 1s when the behavior was present (note: the visualization is qualitative and bin width may differ from those implemented). **(c)** Boolean arrays from the three body movements from approximately 40 trials in the session from (a) (from -15 sec to +5 sec) do not reveal patterns of movement (sum of movements shown as 'blue' curve). (d) the average sum of movements over all sessions in mouse M1 reveals a decrease in body movements in the few seconds prior to lever pull (i.e. time = 0 sec). **(e)** Principal Component Analysis (PCA) on concatenated boolean vectors from all sessions in mouse M1 (note: data for PCA consisted in boolean vectors from -10 sec to 0 sec prior to lever pull; different windows yielded similar results; see Methods) do not reveal obvious clusters in this PCA space (note: clusters may have implied that different body parts have different initiation times, potentially giving rise to sequences).

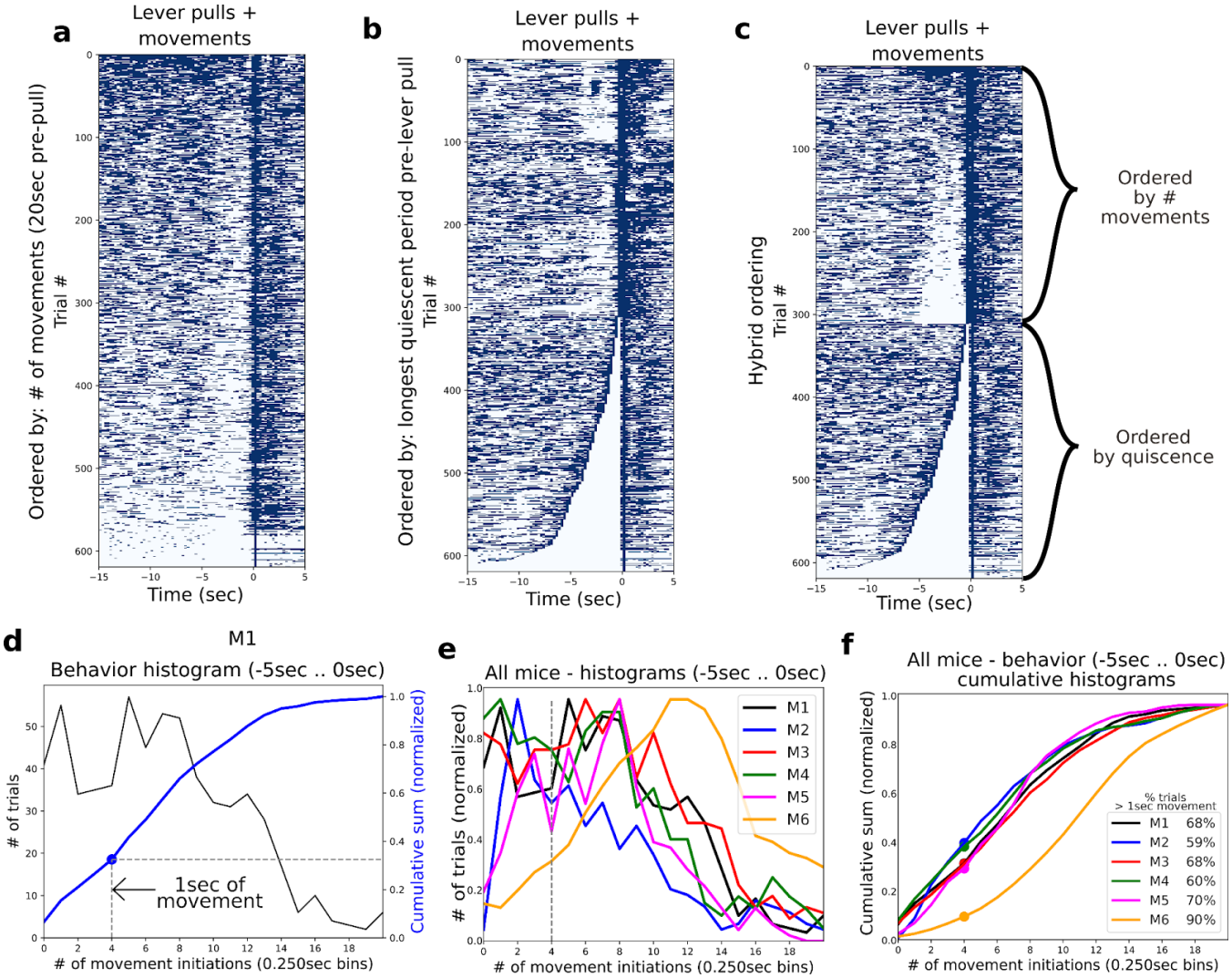

Figure 1, figure supplement 6: Characterizing quiescent periods prior to rewarded lever pulls. (a) Scatter plot of lever pull locations for all (video recorded) trials in mouse M1 ordered by the most active to least active trials in the period of -5sec to 0sec. (b) Same as (a) but trials ordered the duration of quiescence prior to the lever pull. (c) Sames as (a) but ordered first by quiescence and the remainder of trials by # of movements. (d) Widefield [ca] activity for each trial ordered as in (a). (d) Histogram of data in (a) for behaviors occurring in the period of -5sec to 0sec (black) along with the cumulative sum (blue) and the location of the 4 bin (i.e. 1 sec) movement threshold (blue dot). (e) Same as histogram (black curve) in (e) for all mice. (f) Same as cumulative sum (blue curve) in (e) for all mice.

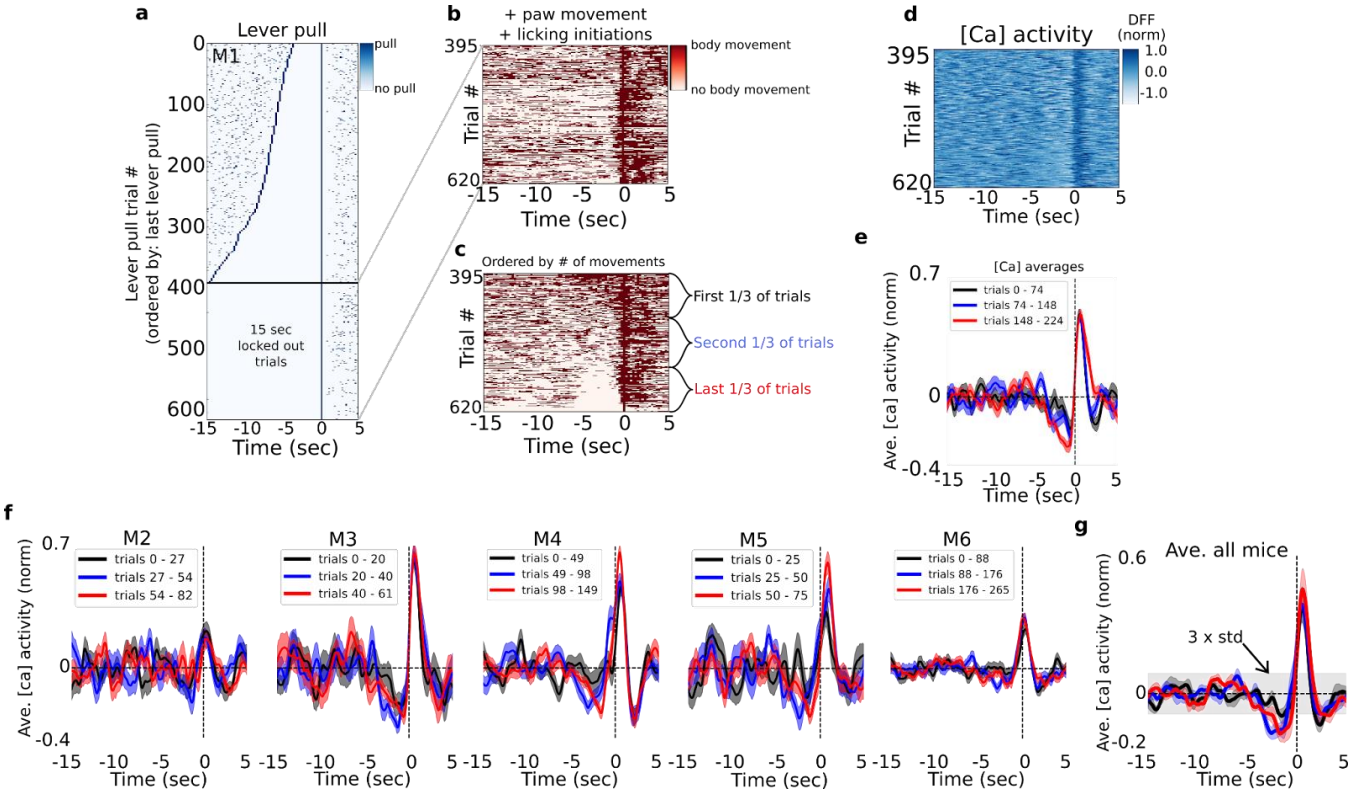

Figure 1, figure supplement 7: Characterizing pre-lever-pull neural activity as a function of body movement. (a) Raster plot of lever pull times for all (video recorded) trials in mouse M1 ordered by the longest pre-pull quiescent (i.e. no-lever pull) period; the bottom 225 rewarded trials were "15sec lockout" trials as they did not have any preceding lever pulls. (b) Left and right paw movements and licking times for the 15sec lever-pull lockout trials shown in (a). (c) Same as (b) but ordered by the most active to least active trials in the period of -5sec to 0sec prior to lever pulls (Note: arranging by longest quiescent periods yielded similar results). (d) Widefield [ca] activity from motor cortex for each trial ordered as in (c). (e) Average neural dynamics for the first, second and last third groups of ordered trials (as in c) for mouse M1 (shading is standard error). (f)-(j) same as (e) but for mice M2-M6. (g) The average of means over all mice (color shading is standard error of the mean; grey shading is the 3 x standard deviation of the signal from -15sec to -5sec; see Methods)

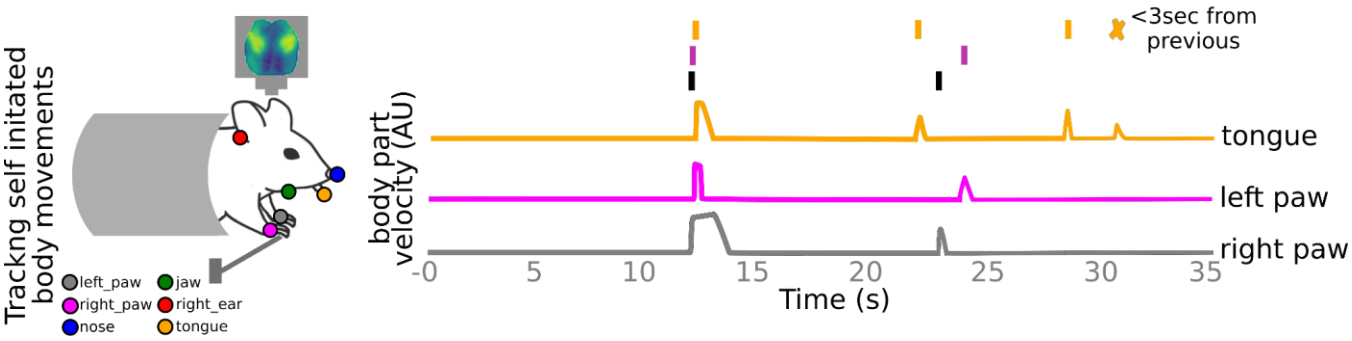

Figure 2 - figure supplement 1: Tracking self-initiated body movements. Markerless pose estimation methods are used to track the locations of left paw, right paw, nose, right year, jaw and tongue. Self-initiated body movements are defined as increases in body part velocities above noise threshold and not preceded by a body movement < 3 sec prior (see also Methods).

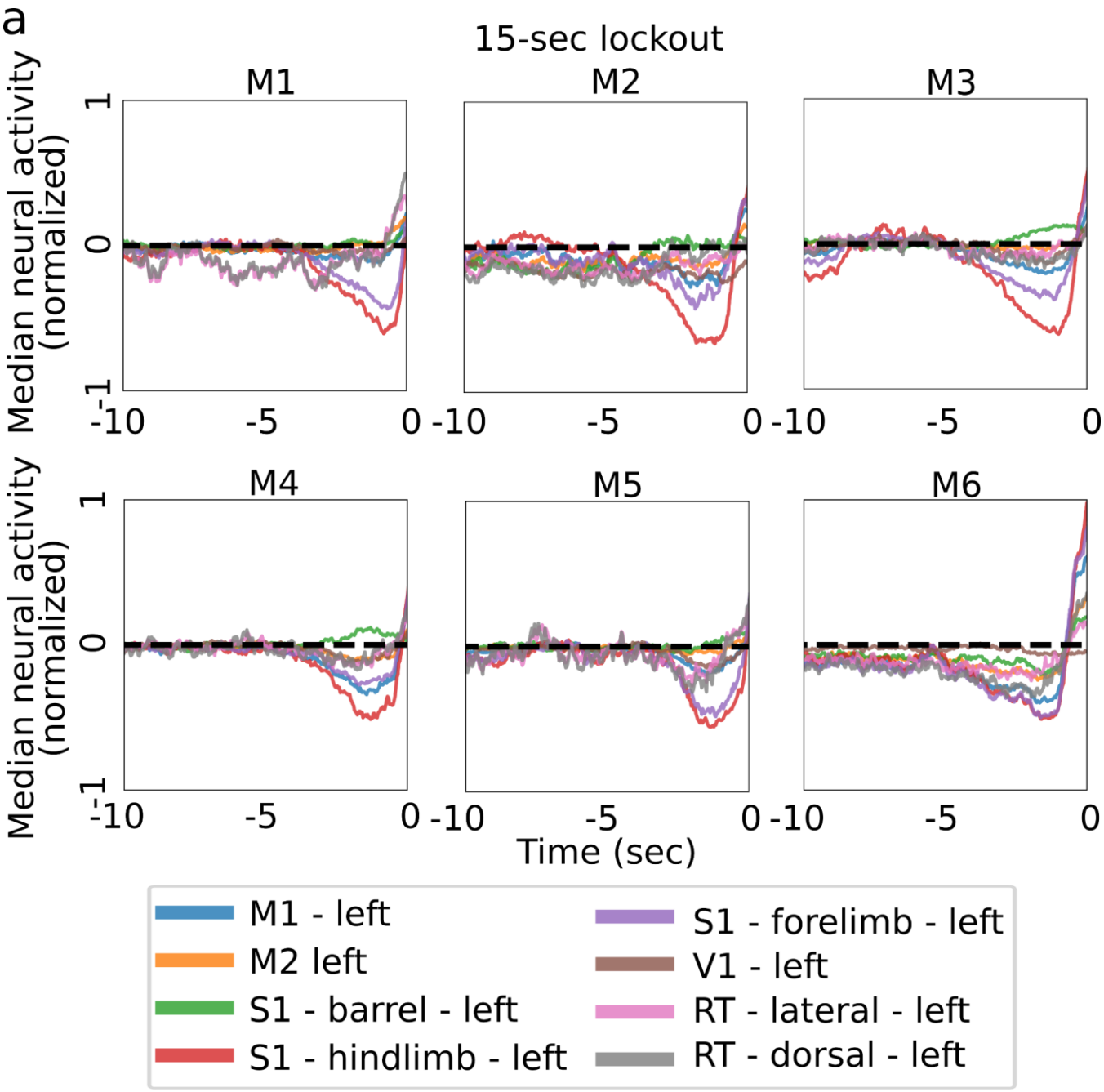

Figure 2 - figure supplement 2: Median neural activity prior to lever pull. (a) Median neural activity in 8 left hemisphere ROIs for all trials (and all sessions) in each mouse using trials not proceeded by other lever-pulls for a period of at least 15 seconds (note: lever was pulled with the right paw).

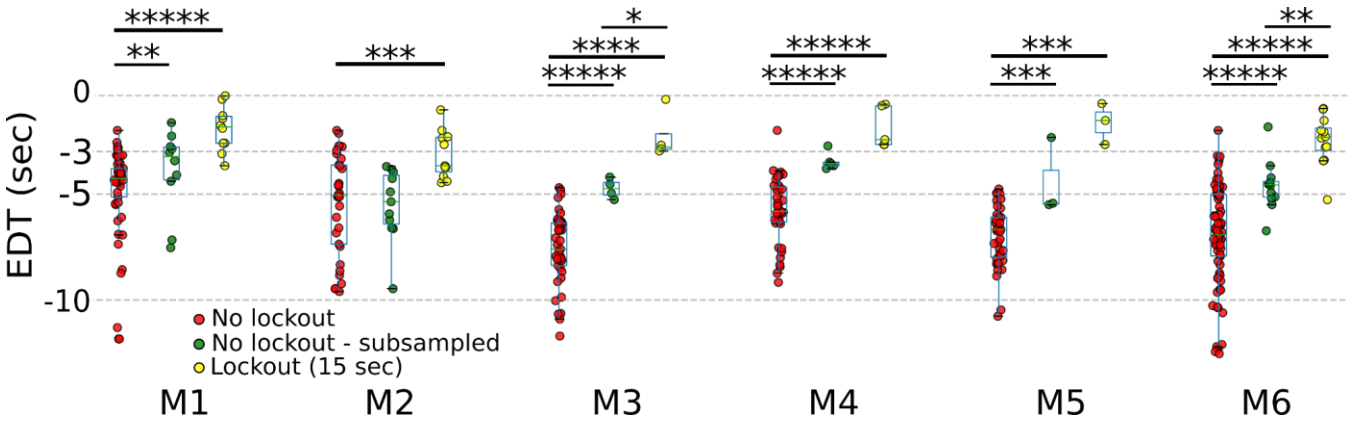

Figure 2 - figure supplement 3: Subsampling non-lockout trials longitudinally leads to an increase in EDTs. EDTs computed from lockout trials (15 sec; yellow) to non-lockout trials (red) to non-lockout trials that uniformly subsampled to match the # of trials in the lockout condition (green). (Pvalues to 5 decimal places: M1: no lockout vs. no lockout subsampled: 0.00171; no lockout vs. no lockout subsampled: 0; no lockout subsampled vs lockout: 0.99446; M2: no lockout vs. no lockout subsampled: 0.53748; no lockout vs. no lockout subsampled: 0.00065; no lockout subsampled vs lockout: 0.21148; M3: no lockout vs. no lockout subsampled: 0.00001; no lockout vs. no lockout subsampled: 0.00001; no lockout subsampled vs lockout: 0.02857; M4: no lockout vs. no lockout subsampled: 0.00001; no lockout vs. no lockout subsampled: 0.00001; no lockout subsampled vs lockout: 0.87302; M5: no lockout vs. no lockout subsampled: 0.00017; no lockout vs. no lockout subsampled: 0.00017; no lockout subsampled vs lockout: 0.6; M6: no lockout vs. no lockout subsampled: 0; no lockout vs. no lockout subsampled: 0; no lockout subsampled vs lockout: 0.00786)

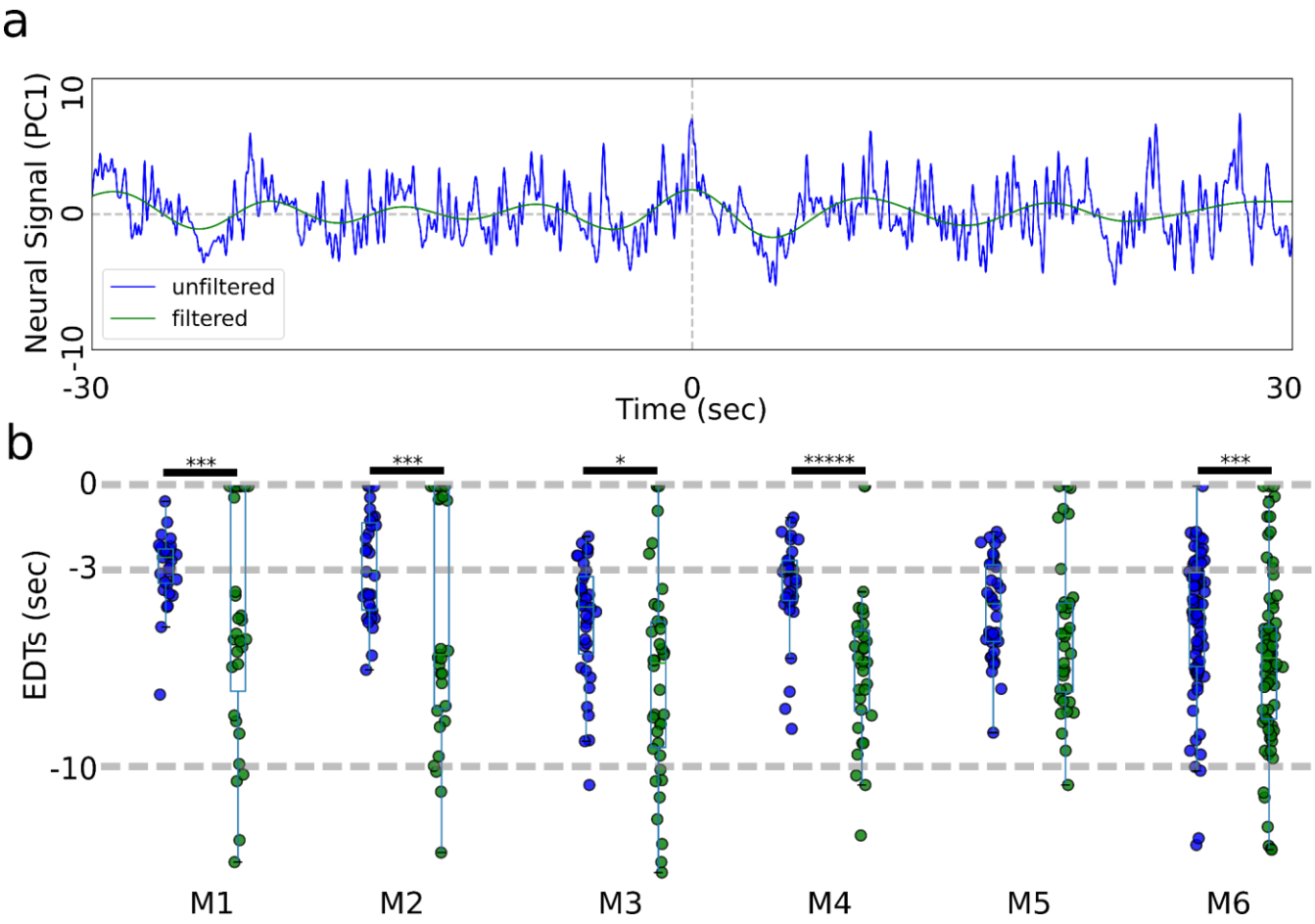

Figure 2 - figure supplement 4: EDTs from low-pass filtered data do not show increased values. **(a)** Panel (a) shows a 60 second segment of signal centered on lever pull before and after filtering (note we use principal components rather than locaNMF ROIs as they are more representative of the raw data). **(b)** EDTs computed using the original unfiltered data (blue) vs filtered data (green) show that all EDTs decrease significantly when removing faster oscillations from the data.

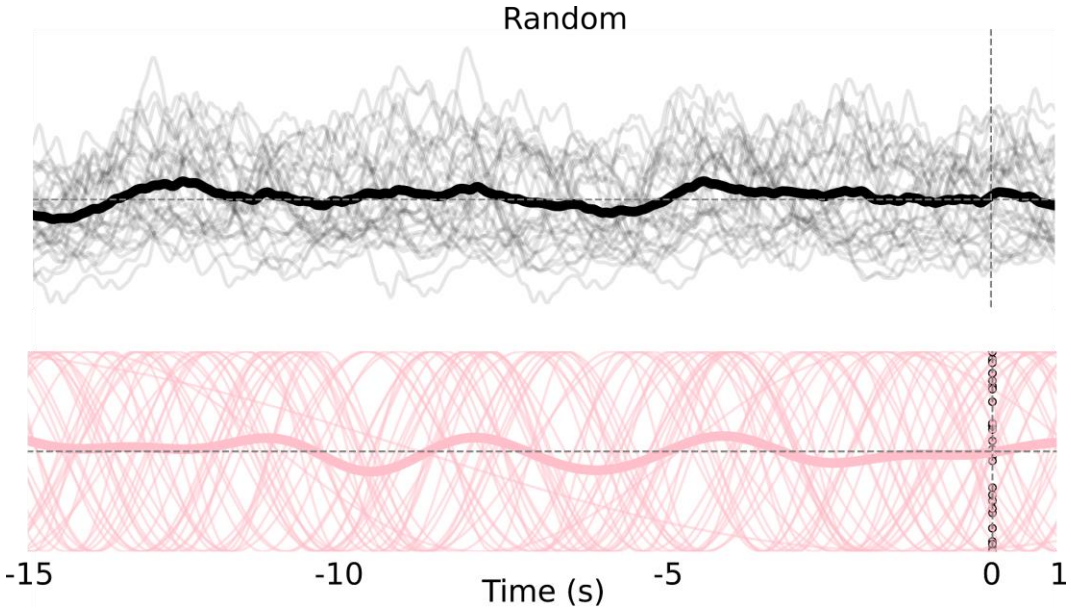

Figure 3 - figure supplement 1: Random controls for slow oscillation sinusoidal fits. Top: single trial neural activity from left somatosensory (limb) cortex (thin black lines) from a session and session average (thick black line). Bottom: sinusoidal fits to data in Top (thin pink lines) and session average (thick pink line).

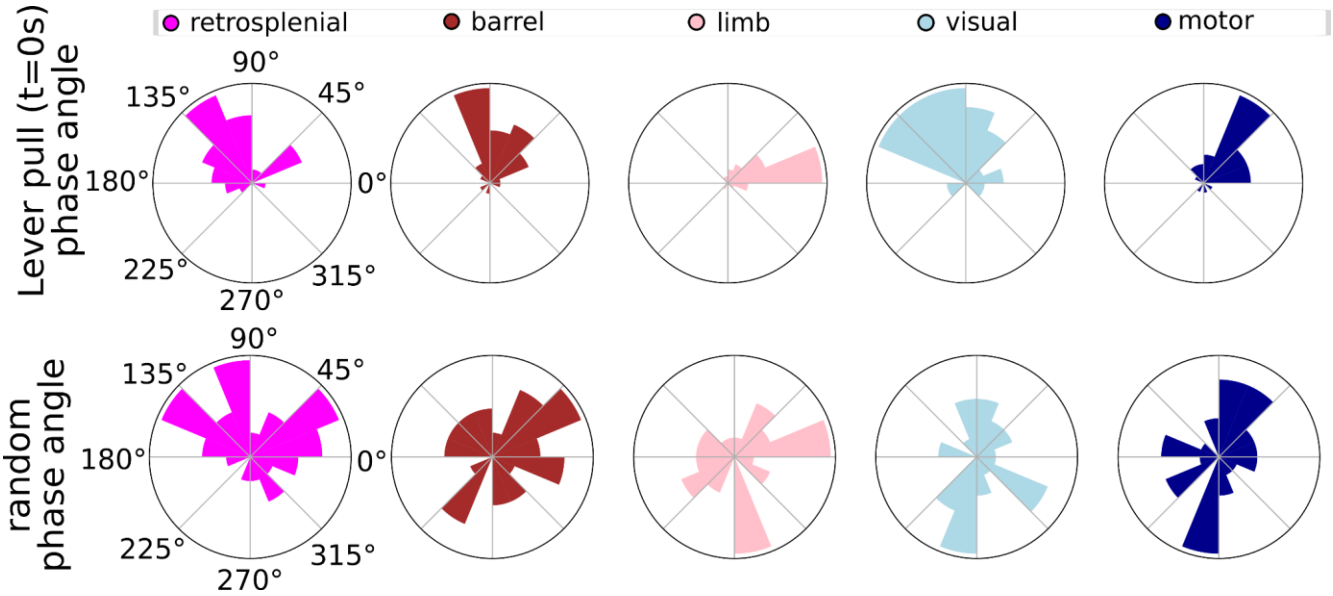

Figure 3 - figure supplement 2: Phases for lever pulls vs. random segments across major cortical areas. Top: single trial phase distributions for retrsponelina, barrel, limb, visual and motor cortex during rewarded lever pull trials in a single session. Bottom: same as Top but for random time points.

References

1. Ashby FG, Turner BO, Horvitz JC. Cortical and basal ganglia contributions to habit learning and automaticity. *Trends Cogn Sci*. 2010;14(5):208-215. doi:10.1016/j.tics.2010.02.001

2. Ball, T., Schreiber, A., Feige, B., Wagner, M., Lücking, C. H., Kristeva-Feige, R., 1999. "The Role of Higher-Order Motor Areas in Voluntary Movement as Revealed by High-Resolution EEG and fMRI". NeuroImage, 10(6), 682–694.

3. Bode, S., Murawski, C., Soon, C. S., Bode, P., Stahl, J., Smith, P. L., 2014. "Demystifying "free will": The role of contextual information and evidence accumulation for predictive brain activity." Neuroscience & Biobehavioral Reviews, 47, 636–645.

4. Bode S, He AH, Soon CS, Trampel R, Turner R, Haynes JD. "Tracking the unconscious generation of free decisions using ultra-high field fMRI.", PLoS One. 2011;6(6):e21612.

5. Brakowski J, Spinelli S, Dörig N, Bosch OG, Manoliu A, Holtforth MG, Seifritz E, "Resting state brain network function in major depression – Depression symptomatology, antidepressant treatment effects, future research", Journal of Psychiatric Research, Volume 92, 2017, Pages 147-159,

6. Chen TW, Wardill TJ, Sun Y, Pulver SR, Renninger SL, Baohan A, Schreiter ER, Kerr RA, Orger MB, Jayaraman V, Looger LL, Svoboda K, Kim DS. Ultrasensitive fluorescent proteins for imaging neuronal activity. Nature. 2013 Jul 18;499(7458):295-300.

7. Churchland MM, Yu BM, Cunningham JP, Sugrue LP, Cohen MR, Corrado GS, Newsome WT, Clark AM, Hosseini P, Scott BB, Bradley DC, Smith MA, Kohn A, Movshon JA, Armstrong KM, Moore T, Chang SW, Snyder LH, Lisberger SG, Priebe NJ, Finn IM, Ferster D, Ryu SI, Santhanam G, Sahani M, Shenoy KV. Stimulus onset quenches neural variability: a widespread cortical phenomenon. Nat Neurosci. 2010 Mar;13(3):369-78.

8. Coe, B., Tomihara, K., Matsuzawa, M., and Hikosaka, O. (2002). Visual and anticipatory bias in three cortical eye fields of the monkey during an adaptive decision-making task. *J. Neurosci*. 22, 5081–5090.

9. Colas JT, Hsieh PJ. "Pre-existing brain states predict aesthetic judgments". Hum Brain Mapp. 2014 Jul;35(7):2924-34.

10. Cunnington, R., Windischberger, C., Deecke, L., Moser, E., 2002. "The Preparation and Execution of Self-Initiated and Externally-Triggered Movement: A Study of EventRelated fMRI.", NeuroImage, 15(2), 373–385.

11. Custers, R., Aarts, H., 2010. "The unconscious will: how the pursuit of goals operates outside of conscious awareness". Science 329, 47–50.

12. Deecke, L., Grözinger, B., Kornhuber, H. H., 1976. Voluntary finger movement in man: cerebral potentials and theory. Biological cybernetics, 23(2), 99–119.

13. Deecke, L., Kornhuber, H. H., 1978. An electrical sign of participation of the mesial "supplementary" motor cortex in human voluntary finger movement. Brain Research, 159(2), 473–476.

14. Deecke, L. (2012). "There Are Conscious and Unconscious Agendas in the Brain and Both Are Important—Our Will Can Be Conscious as Well as Unconscious.", Brain Sciences, 2(4), 405–420.

15. Dijksterhuis, A., Bos, M.W., Nordgren, L.F., van Baaren, R.B., 2006. "On making the right choice: the deliberation-without-attention effect". Science 311, 1005–1007.

16. Dijksterhuis A, Aarts H (2010) "Goals, attention and (Un)consciousness". Annu Rev Psychol 61:467–490.

17. Ding, L., and Hikosaka, O. (2006). Comparison of reward modulation in the frontal eye field and caudate of the macaque. *J. Neurosci*. 26, 6695–6703.

18. Fried, I., Mukamel, R., Kreiman, G., 2011. "Internally Generated Preactivation of Single Neurons in Human Medial Frontal Cortex Predicts Volition". Neuron, 69(3), 548–562.

19. Gold JI, Shadlen MN. "The neural basis of decision making". Annu Rev Neurosci. 2007;30:535–574.

20. Guggisberg, A. G., Mottaz, A., 2013. "Timing and awareness of movement decisions: does consciousness really come too late?", Frontiers in Human Neuroscience, 7.

21. Haggard, P., 2008. "Human volition: towards a neuroscience of will", Nature Reviews Neuroscience, 9(12), 934–946.

22. Haggard, P., Eimer, M., 1999. "On the relation between brain potentials and the awareness of voluntary movements". Experimental Brain Research, 126(1), 128–133.

23. He BJ, Raichle ME. The fMRI signal, slow cortical potential and consciousness. Trends Cogn Sci. 2009 Jul;13(7):302-9.

24. Heekeren, H.R., Marret, S., Ungerleider, L.G., 2008. "The neural systems that mediate human perceptual decision making". Nat. Rev. Neurosci. 9, 467–479.

25. Hyland B. Neural activity related to reaching and grasping in rostral and caudal regions of rat motor cortex. Behav Brain Res. 1998 Aug;94(2):255-69.

26. International Brain Laboratory (IBL), Aguillon-Rodriguez V, Angelaki D, Bayer H, Bonacchi N, Carandini M, Cazettes F, Chapuis G, Churchland AK, Dan Y, Dewitt E, Faulkner M, Forrest H, Haetzel L, Häusser M, Hofer SB, Hu F, Khanal A, Krasniak C, Laranjeira I, Mainen ZF, Meijer G, Miska NJ, Mrsic-Flogel TD, Murakami M, Noel JP, Pan-Vazquez A, Rossant C, Sanders J, Socha K, Terry R, Urai AE, Vergara H, Wells M, Wilson CJ, Witten IB, Wool LE, Zador AM. "Standardized and reproducible measurement of decision-making in mice". Elife. 2021 May 20;10:e63711.

27. Isomura Y, Takekawa T, Harukuni R, Handa T, Aizawa H, Takada M, Fukai T. Reward-modulated motor information in identified striatum neurons. J Neurosci. 2013 Jun 19;33(25):10209-20.

28. Jahanshahi, M., Hallett, M., 2003. “The Bereitschaftspotential: What Does It Measure and where Does It Come from?” In M. Jahanshahi & M. Hallett (Hrsg.), The Bereitschaftspotential (S. 1–17). Springer US.

29. Jo HG, Hinterberger T, Wittmann M, Borghardt TL, Schmidt S. “Spontaneous EEG fluctuations determine the readiness potential: is preconscious brain activation a preparation process to move?” Exp Brain Res. 2013 Dec;231(4):495-500.

30. Kagaya K, Takahata M. “Readiness discharge for spontaneous initiation of walking in crayfish”. J Neurosci. 2010 Jan 27;30(4):1348-62.

31. Klemm, W., 2010. “Free will debates: Simple experiments are not so simple.” Advances in Cognitive Psychology, 6(-1), 47–65.

32. Kornhuber, H. H. and Deecke, L. (1964) “Hirnpotentialänderungen beim Menschen vor und nach Willkürbewegungen,dargestellt mit Magnetband-Speicherung und Rückwärtsanalyse”.Pflügers Arch.281, 52.

33. Kornhuber, H.H., Deecke, L.”Hirnpotentialänderungen bei Willkürbewegungen und passiven Bewegungen des Menschen: Bereitschaftspotential und reafferente Potentiale”. Pflügers Arch. 284, 1–17 (1965).

34. Lages, M., Boyle, S.C., Jaworska, K., 2013. “Flipping a coin in your head without monitoring outcomes? Comments on predicting free choices and a demo program”. Front. Psychol. 4, 925

35. Lang, W., 2003. “Surface Recordings of the Bereitschaftspotential in Normals.”, In M. Jahanshahi & M. Hallett (Hrsg.), The Bereitschaftspotential (S. 19–34). Springer US. Abgerufen von http://link.springer.com/chapter/10.1007/978-1-4615-0189-3_2.

36. Lavazza A. “Free Will and Neuroscience: From Explaining Freedom Away to New Ways of Operationalizing and Measuring It”. *Front Hum Neurosci*. 2016;10:262. Published 2016 Jun 1.

37. Lee IH, Assad JA. “Putaminal activity for simple reactions or self-timed movements”. J Neurophysiol. 2003; 89:2528–2537.

38. Libet, B., Gleason, C. A., Wright, E. W., Pearl, D. K., 1983. “Time of Conscious Intention to Act in Relation to Onset of Cerebral-Activity (Readiness-Potential) - the Unconscious Initiation of A Freely Voluntary Act”. Brain, 106(SEP), 623–642.

39. Lin Q, Manley J, Helmreich M, Schlumm F, Li JM, Robson DN, Engert F, Schier A, Nöbauer T, Vaziri A. Cerebellar Neurodynamics Predict Decision Timing and Outcome on the Single-Trial Level. Cell. 2020 Feb 6;180(3):536-551.e17.

40. Lysaker PH, Pattison ML, Leonhardt BL, Phelps S, Vohs JL. “Insight in schizophrenia spectrum disorders: relationship with behavior, mood and perceived quality of life, underlying causes and emerging treatments.” World Psychiatry. 2018 Feb;17(1):12-23.

41. Madisen L, Garner AR, Shimaoka D, Chuong AS, Klapoetke NC, Li L, van der Bourg A, Niino Y, Egolf L, Monetti C, et al. Transgenic mice for intersectional targeting of neural sensors and effectors with high specificity and performance. Neuron. 2015; 85:942–958.

42. Maimon G, Assad JA. “A cognitive signal for the proactive timing of action in macaque LIP”. Nat Neurosci. 2006;9:948–955.

43. Maoz, U., Mudrik, L., Rivlin, R., Ross, I., Mamelak, A., & Yaffe, G. (2015) “On reporting the onset of the intention to move”. In A. R. Mele (Ed.), Surrounding free will: Philosophy, psychology, neuroscience (pp. 184-202). New York, NY: Oxford University Press.

44. Maoz, U., Yaffe, G., Koch, C., & Mudrik, L. (2019). Neural precursors of deliberate and arbitrary decisions in the study of voluntary action. Elife, 8, e39787.

45. Mathis, A., Mamidanna, P., Cury, K.M. et al. DeepLabCut: markerless pose estimation of user-defined body parts with deep learning. Nat Neurosci 21, 1281–1289 (2018).

46. Mudrik, L., Levy, D. J., Gavenas, J., & Maoz, U. (2020). “Studying volition with actions that matter: Combining the fields of neuroeconomics and the neuroscience of volition”. Psychology of Consciousness: Theory, Research, and Practice, 7(1), 67.

47. Murakami M, Vicente MI, Costa GM, Mainen ZF. “Neural antecedents of self-initiated actions in secondary motor cortex”. Nat Neurosci. 2014 Nov;17(11):1574-82. Epub 2014 Sep 28.

48. Murakami M, Shteingart H, Loewenstein Y, Mainen ZF. Distinct Sources of Deterministic and Stochastic Components of Action Timing Decisions in Rodent Frontal Cortex. Neuron. 2017 May 17;94(4):908-919.e7.

49. Musall S, Kaufman MT, Juavinett AL, Gluf S, Churchland AK. “Single-trial neural dynamics are dominated by richly varied movements". Nat Neurosci. 2019 Oct;22(10):1677-1686.

50. Najafi F, Churchland AK, “Perceptual Decision-Making: A Field in the Midst of a Transformation. (2018) Neuron 100 (2), 453-462

51. Northoff G., "Paradox of slow frequencies" - Are slow frequencies in upper cortical layers a neural predisposition of the level/state of consciousness (NPC)? Conscious Cogn. 2017 Sep;54:20-35.

52. Odoemene O, Pisupati S, Nguyen H, Churchland AK. “Visual evidence accumulation guides decision-making in unrestrained mice”. The Journal of Neuroscience, 2018; 3478-17.

53. Park HD, Barnoud C, Trang H, Kannape OA, Schaller K, Blanke O. “Breathing is coupled with voluntary action and the cortical readiness potential.” Nat Commun. 2020 Feb 6;11(1):289.

54. Ratcliff, R. (1978). “A theory of memory retrieval”. Psychological Review, 85(2), 59-108.

55. Ratcliff R, McKoon G. “The diffusion decision model: theory and data for two-choice decision tasks”. *Neural Comput*. 2008;20(4):873-922. doi:10.1162/neco.2008.12-06-420

56. Romo R, Schultz W (1986) Discharge activity of dopamine cells in monkey midbrain: comparison of changes related to triggered and spontaneous movements. Soc Neurosci Abstr 12: 207

57. Romo R, Schultz W. Dopamine neurons of the monkey midbrain: contingencies of responses to active touch during self-initiated arm movements. J Neurophysiol. 1990 Mar;63(3):592-606. doi: 10.1152/jn.1990.63.3.592. PMID: 2329363.

58. Saxena S, Kinsella I, Musall S, Kim SH, Meszaros J, Thibodeaux DN, Kim C, Cunningham J, Hillman EMC, Churchland A, Paninski L. “Localized semi-nonnegative matrix factorization (LocaNMF) of widefield calcium imaging data”. PLoS Comput Biol. 2020 Apr 13;16(4):e1007791.

59. Schlegel, A., Alexander, P., Sinnott-Armstrong, W., Roskies, A., Tse, P. U., Wheatley, T., 2013. “Barking up the wrong free: readiness potentials reflect processes independent of conscious will.” Experimental Brain Research, 229(3), 329–335.

60. Schmidt S, Jo HG, Wittmann M, Hinterberger T. 'Catching the waves' - slow cortical potentials as moderator of voluntary action. Neurosci Biobehav Rev. 2016 Sep;68:639-650.

61. Schurger, A., Sitt, J. D., Dehaene, S., 2012. “An accumulator model for spontaneous neural activity prior to self-initiated movement”. Proceedings of the National Academy of Sciences, 109(42), E2904–E2913.

62. Schurger, A., Mylopoulos, M., & Rosenthal, D. (2016). “Neural Antecedents of Spontaneous Voluntary Movement: A New Perspective.”, Trends in Cognitive Sciences, 20(2), 77–79.

63. Shibasaki, H., Hallett, M., 2006. “What is the Bereitschaftspotential?”, Clinical Neurophysiology, 117(11), 2341–2356.

64. Silasi G, Xiao D, Vanni MP, Chen ACN, Murphy TH, “Intact skull chronic windows for mesoscopic wide-field imaging in awake mice” J. Neurosci. Methods, 267 (2016), pp. 141-149

65. Silasi G, Boyd JD, Bolanos F, LeDue JM, Scott SH, Murphy TH, “Individualized tracking of self-directed motor learning in group-housed mice performing a skilled lever positioning task in the home cage”, Journal of Neurophysiology 2018 119:1, 337-346

66. Sinnott-Armstrong W, nadel l (eds) (2010) “Conscious will and responsibility”, 1st edn. Oxford University Press, USA.

67. Sirigu, A., Daprati, E., Ciancia, S., Giraux, P., Nighoghossian, N., Posada, A., Haggard, P., 2004. “Altered awareness of voluntary action after damage to the parietal cortex.”, Nature Neuroscience, 7(1), 80–84.

68. Soon, C. S., Brass, M., Heinze, H. J., and Haynes, J. D. (2008). “Unconscious determinants of free decisions in the human brain”. Nat. Neurosci. 11, 543–545.

69. Soon CS, He AH, Bode S, Haynes JD. “Predicting free choices for abstract intentions.”, Proc Natl Acad Sci U S A. 2013 Apr 9;110(15):6217-22.

70. Travers E, Friedemann M, Haggard P (2021) “The Readiness Potential reflects planning-based expectation, not uncertainty, in the timing of action”, Cognitive Neuroscience, 12:1, 14-27.

71. Tusche, A., Bode, S., Haynes, J.D., 2010. “Neural responses to unattended products predict later consumer choices”. J. Neurosci. 30 (23), 8024–8031.

72. Vanni MP, Murphy TH, “Mesoscale transcranial spontaneous activity mapping in GCaMP3 transgenic mice reveals extensive reciprocal connections between areas of somatomotor cortex”, J. Neurosci., 34 (48) (2014), pp. 15931-15946

73. Vierkant T, Deutschländer R, Sinnott-Armstrong W, Haynes JD. “Responsibility Without Freedom? Folk Judgements About Deliberate Actions”. Front Psychol. 2019;10:1133. Published 2019 May 21.

74. Wander JD, Blakely T, Miller KJ, Weaver KE, Johnson LA, Olson JD, Fetz EE, Rao RP, Ojemann JG. “Distributed cortical adaptation during learning of a brain-computer interface task”. Proc Natl Acad Sci U S A. 2013 Jun 25;110(26):10818-23.

75. Wegner DM (2002) the Illusion of conscious will. MIt Press, Cambridge, MA.

76. Xiao D, Vanni MP, Mitelut CC, et al. Mapping cortical mesoscopic networks of single spiking cortical or sub-cortical neurons. *Elife*. 2017;6:e19976.

Table 1. Lever pull statistics

Animal ID	# of behavior sessions*	# of video sessions*	Median # rewarded pulls / session	Median # unrewarded pulls / session
M1	69	30	16	14
M2	42	12	34	14
M3	42	11	42	135
M4	46	10	33	111
M5	42	11	38	116
M6	109	70	45	35

***** Total numbers reported include also rejected sessions due to insufficient trials (see also Methods).